

NASA Research Grant

NRG - 305

May 1965

FACILITY FORM 602

N65-33276

(ACCESSION NUMBER)

(THRU)

75

1

(PAGES)

(CODE)

CR 64805

20

(NASA CR OR TMX OR AD NUMBER)

(CATEGORY)

FINAL REPORT

INVESTIGATION OF ATMOSPHERIC PROPERTIES BASED
UPON EVALUATION OF INFRARED RADIATION
DATA OBTAINED FROM TIROS SATELLITES

Erhard Raschke
Irmhild Tannhäuser

Meteorologisches Institut
der Universität München

Institutsvorstand Prof. Dr. F. Möller

GPO PRICE \$

CSFTI PRICE(S) \$

Hard copy (HC) 3.00

Microfiche (MF) .75

ff 653 July 65

The research reported in this document
has been sponsored by the
NATIONAL AERONAUTICS AND SPACE ADMINISTRATION (NASA)
Washington 25, D.C.

NASA Research Grant

NsG - 305

May 1965

F I N A L R E P O R T

INVESTIGATION OF ATMOSPHERIC PROPERTIES BASED
UPON EVALUATION OF INFRARED RADIATION
DATA OBTAINED FROM TIROS SATELLITES

Erhard Raschke
Irmhild Tannhäuser

Meteorologisches Institut
der Universität München

Institutsvorstand Prof. Dr. F. Möller

The research reported in this document
has been sponsored by the
NATIONAL AERONAUTICS AND SPACE ADMINISTRATION (NASA)
Washington 25, D.C.

Part I : Evaluation of TIROS III Radiation
Data - Quasiglobal Presentation
of the Mean Relative Humidity of
the Upper Troposphere and of the
Surface Temperature.

Part II : Influence of Minor Constituents
on the Outgoing Radiation.

Part I: Evaluation of TIROS III Radiation
Data - Quasiglobal Presentation
of the Mean Relative Humidity of
the Upper Troposphere and of the
Surface Temperature.

A b s t r a c t :

B3276

The measured values of the TIROS III satellite from the first 6 days after the launch (July, 12. - July, 17. 1961) have been collected in quasiglobal presentations. In the same way are also collected values of the mean relative humidity of the upper troposphere and of the temperature of the emitting surface (cloud or ground), which were derived from the radiation data of the channels 1 ($5.8 \mu - 6.8 \mu$) and 2 ($8 \mu - 13 \mu$).

Author

C O N T E N T S

	page
1. Introduction	1
2. Quasiglobal presentations of infrared radiation data	3
3. Determination of the mean relative humidity of the upper troposphere and of the surface tempera- ture of the emitting surface	3
4. Quasiglobal presentation of the mean relative hu- midity of the upper troposphere, of the surface temperature, and of the albedo	6
5. Concluding remarks	14
6. References	16
7. Appendix : Quasiglobal presentations of the TIROS III radiation data measured during the orbits 1 - 77 (July, 12 - July, 17 1961)	18

1. Introduction:

During the past two years a method has been developed for the determination of the mean relative humidity of the upper troposphere and of the temperature of emitting surfaces from satellite measurements of the thermal radiation emerging into space. Preliminary evaluations have been carried out with radiation data of the TIRCS III meteorological satellite from parts of several orbits [1,2].

It will be tried here to collect the measured values and the parameters of the atmospheric structure derived from them for all orbits of single days in a quasiglobal presentation. These presentations may give a survey of the radiation field of the earth as it has been measured from the TIROS III satellite.

It has been reported on first attempts by RASCHKE [3] and BANDEEN [4] and afterwards by L. ALLISSON et al. [5]. ALLISSON and his collaborators compared the upward radiation flux, which was measured from TIROS III in the window region between 8 and 12 microns with several characteristics of the synoptic weather analysis.

The radiation emitted and reflected from the earth and its atmosphere into space has been measured from TIRCS III within five spectral regions (Table 1, see also [6]).

	channel	spectral region
longwave radiation	1	5.8 μ - 6.8 μ
	2	8 μ - 13 μ
	4	7.5 μ - 32.5 μ
shortwave radiation	3	0.2 μ - 6.0 μ
	5	0.55 μ - 0.75 μ

Table 1: Spectral regions of the TIROS III five channel medium resolution radiometer [6].

The shortwave radiation reflected from the earth and its atmosphere can be measured only over the dayside of the globe. Assuming that the spectral distribution of both the extraterrestrial and the reflected solar radiation is the same, values of the mean diffuse reflectivity (albedo) of the area "viewed" by the satellite can easily be determined. Over cloudy and desert areas these albedo values are high, whereas over the open sea low values have been found (Chapter 4).

In the spectral region of channel 1 only thermal radiation emitted from the water vapor of the upper troposphere and of the stratosphere in its 6.3μ - band can penetrate up to the satellite [1,2]. Therefore, equivalent black body temperatures (in short equivalent temperatures) determined from the measured radiation fluxes are representative for the mean temperature and the content of water vapor of these emitting layers. It has been shown [1,2,7], that under the assumption of model stratifications of the atmosphere the radiation data of channel 1 are a measure for the mean relative humidity of the upper troposphere.

The sensitivity regions of the channels 2 and 4 contain the weak absorbing water vapor window between 8 and 12 microns. Thus the measured radiation fluxes of those channels are nearly a function of the temperature of the emitting surfaces. Since channel 4 also receives radiation emitted in the spectral region of the strong absorbing 15 micron band of CO_2 from high and cold layers its equivalent temperatures are lower than those of channel 2. Earlier research [1,2,8], however, has proved that the measured data of both channels show a narrow correlation.

As it has been proposed by MÖLLER [9] the radiation data of channel 1 which were measured simultaneously with those of channel 2, will be used as a measure of that water vapor mass the absorption of which must be taken into account if

the surface temperature will be determined from channel 2. This evaluation method has been discussed in detail by MÖLLER and RASCHKE [1].

2. Quasiglobal presentations of infrared radiation data.

For the first 6 days (July, 12. - July, 17. 1961) after the launch of TIROS III quasiglobal maps of the daily "synoptic" radiation field have been drawn from averages of all data measured within geographic fields of 4 degrees longitude and 4 degrees latitude. These maps are shown in the appendix. They were obtained from all measured data. Only those data were omitted which were measured with a nadir angle larger than 50 degrees, and data with a minus sign [6, page 6]. Furthermore, data of all those points were omitted where channel 1 measured equivalent temperatures smaller than 215 °K and channel 2 simultaneously larger ones than 225 °K. As it can be shown by model calculations the equivalent temperatures of both channels in this order of magnitude are nearly equal. However, due to system noise data of channel 1 in this size region showed a large scatter and a high inaccuracy.

The maps obtained in this way represent a quasi-synoptic survey of the radiation field in different spectral regions, which was measured daily from TIROS III between 60 degrees Northern and Southern latitude.

3. Determination of the mean relative humidity of the upper troposphere and of the surface temperature of emitting surfaces.

As it has been stated above, the measured values of channel 2 are a measure for the temperatures of the emitting surface (clouds or ground) on the earth after some corrections

have been applied for the water vapor absorption. The values measured simultaneously by channel 1 are a measure for the mean relative humidity of the upper troposphere and therefore also for the water vapor mass, the absorption of which must be taken into account, if the surface temperature will be determined from radiation data of channel 2.

Both quantities, the relative humidity and the surface temperature, can therefore be found by comparing the measured radiation fluxes with those computed for the same spectral regions for model stratifications of the atmosphere. This method has been discussed in detail in [1] and in [2]. Therefore, only a short description of it will be given here:

The upward outgoing radiation fluxes in the channels 1 and 2 have been calculated for two model atmospheres. One of them is representative for mean conditions in midlatitude regions (atmosphere 1) and the other for tropical regions (atmosphere 2). The main characteristics of the temperature profiles of both are compiled in Table 2.

	atmosphere 1	atmosphere 2
surface temperature	+ 15.0 °C	+ 35.0 °C
temperature gradient in the troposphere	- 6.5 °/km	- 6.5 °/km
in the stratosphere	+ 3.0 °/km	+ 3.0 °/km
temperature and height of the tropopause	-56.5 °C at 11km	-75.0 °C at 16.9km
height of the upper boundary of the isothermal part of the lower stratosphere	25.0 km	18.5 km

Table 2: Main characteristics of the temperature profiles of the two model atmospheres.

The absorbing masses of CO_2 have been determined assuming 0.03 % per Vol., those for O_3 from mean vertical distributions [10]. The water vapor masses have been determined for different values of the relative humidity of the troposphere, which has been assumed to be constant in the troposphere, and for a vertical water vapor distribution in the stratosphere after GUTNICK [11], which remained unchanged in all calculations. In order to take into account changes of the surface temperature, radiation fluxes have been computed for different heights of a dense and black emitting cloud layer in the troposphere. From these radiation flux calculations curves of constant equivalent temperature for each channel could be drawn in diagrams in dependence on the relative humidity and on the surface temperature. The coordinates of points of intersection of curves of both channels, the parameters of which are given the measured values, give then the desired values of the mean relative humidity and the surface temperature.

These model assumptions do not represent the actual state of the atmosphere. Therefore, the results found by these evaluations might be considered as equivalent values which are only valid for idealized conditions. It could be shown by some estimations [1,2], that deviations of the actual stratification from the assumed models can cause results which are higher or lower than actual values.

The dependence of the measured radiation flux from the nadir angle N was regarded for by comparison with radiation fluxes calculated for nadir angles $N = 0, 40$ and 50 degrees for both model atmospheres. In the evaluation procedure the measured values have been divided into three groups according to their nadir angle ($0 \leq N \leq 29$, $30 \leq N \leq 44$, $45 \leq N \leq 50$ degrees). The relative humidities and the surface temperatures then have been determined with the correspondend diagram. For all data measured between geographical latitudes of 40 degrees North and 40 degrees South diagrams

for the atmosphere 2 have been used and for all other data those for atmosphere 1. For that entire evaluation procedure a computer program has been used.

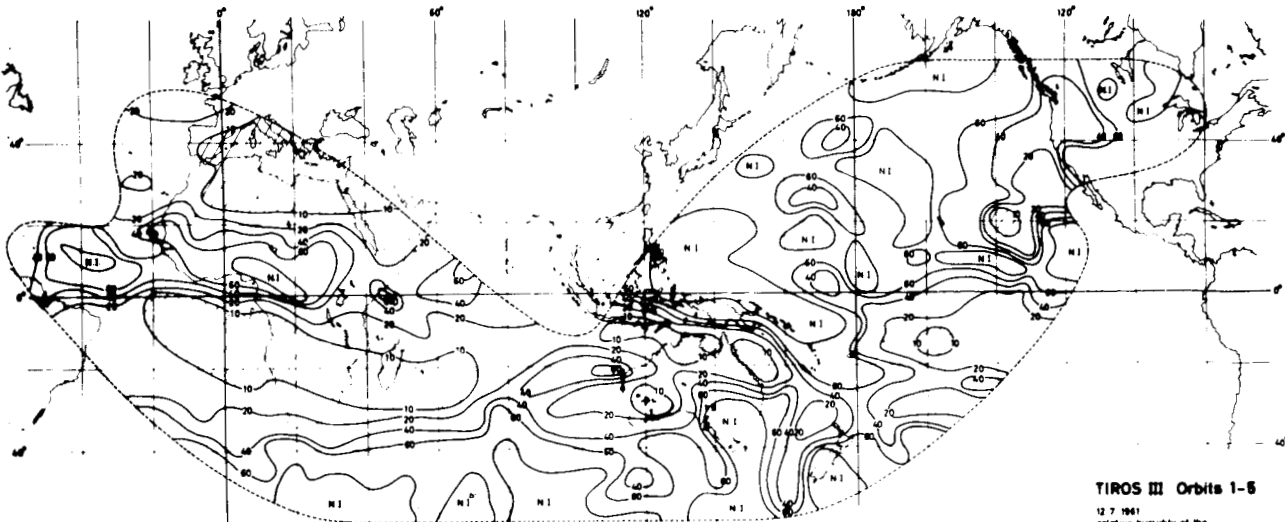
4. Quasiglobal presentation of the mean relative humidity of the upper troposphere, of the surface temperature, and of the albedo.

The maps of the mean relative humidity of the upper troposphere, of the surface temperature, and of the albedo are shown in Figs 1 - 18, pages 7 - 12.

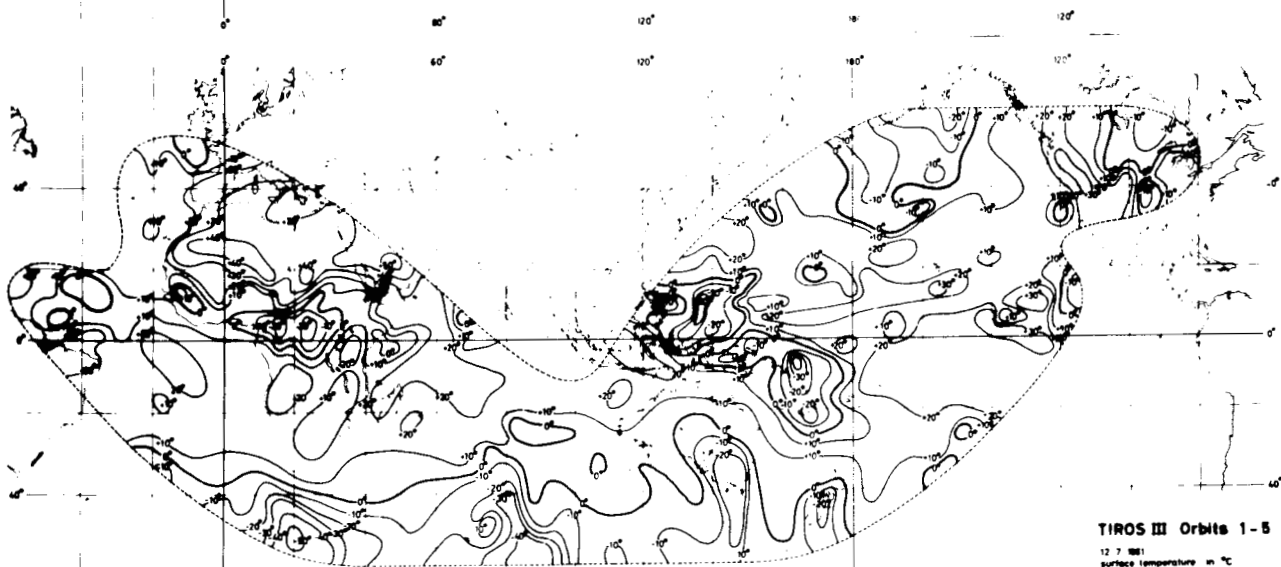
Low values of the mean relative humidity occur in subtropical regions at both sides of the equator. As it has been stated in 1, the relative humidity seems to increase as the surface temperature decreases. This fact could lead to the assumption that over cloudy areas the relative humidity of the upper troposphere is higher than over cloudless areas.

Values of the relative humidity of more than 100 % have been found over those areas, which are designed in the maps with N. I. (that means, no intersection of curves of constant equivalent temperature of the channels 1 and 2 within the region of validity of the evaluation diagrams). These areas coincide with those for which very low surface temperatures have been found. The presence of these areas demonstrates the limitations of the evaluation method, since too many simplifications on the atmospheric stratification may have had to be introduced into the model atmosphere. As it has been discussed in detail in [1] and [2], mainly thin cirrus clouds or dust layers near the tropopause, also a colder and moister stratosphere can cause that apparent relative humidities of more than 100 % will be found from the radiation data of channel 1.

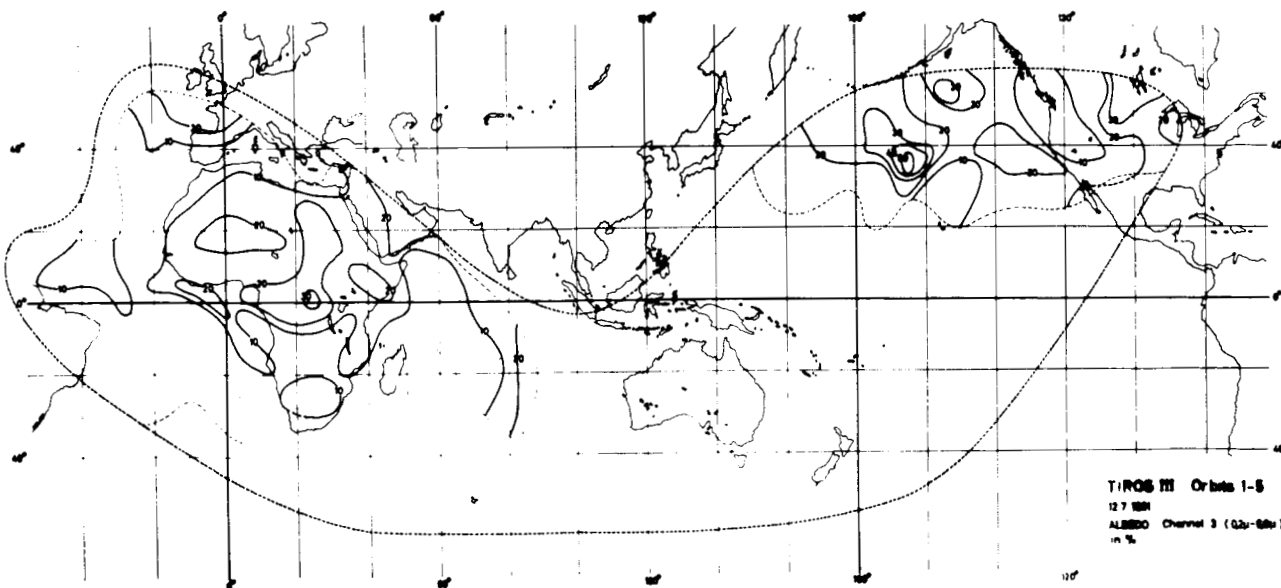
From all humidity values, determined from the radiation data of the orbits 1 - 5 latitudinal averages have been



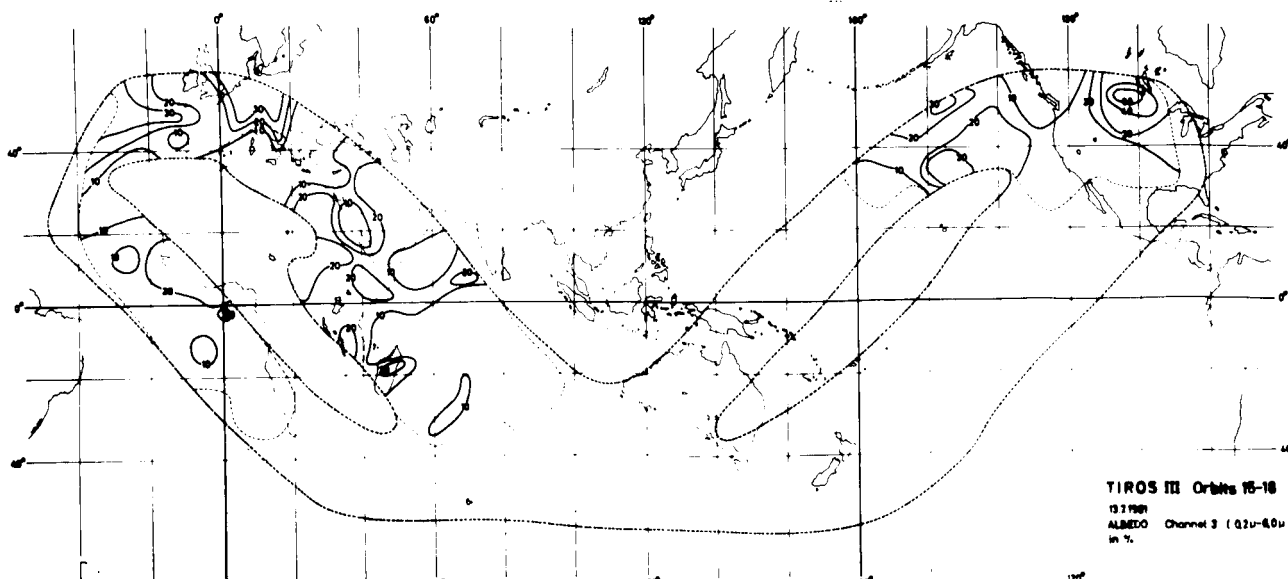
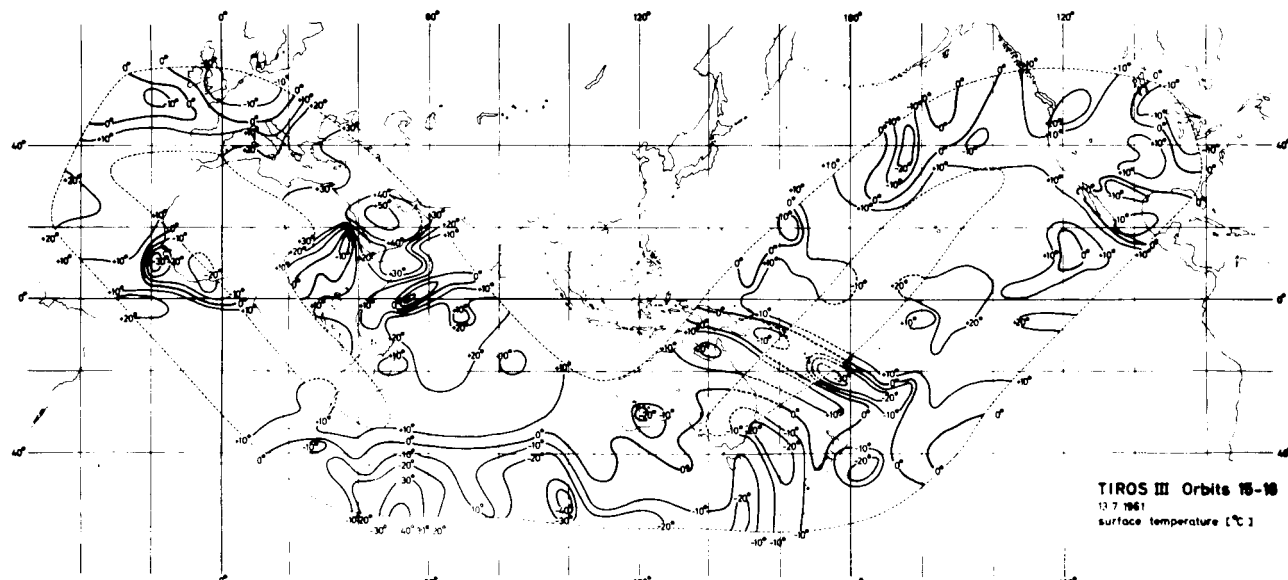
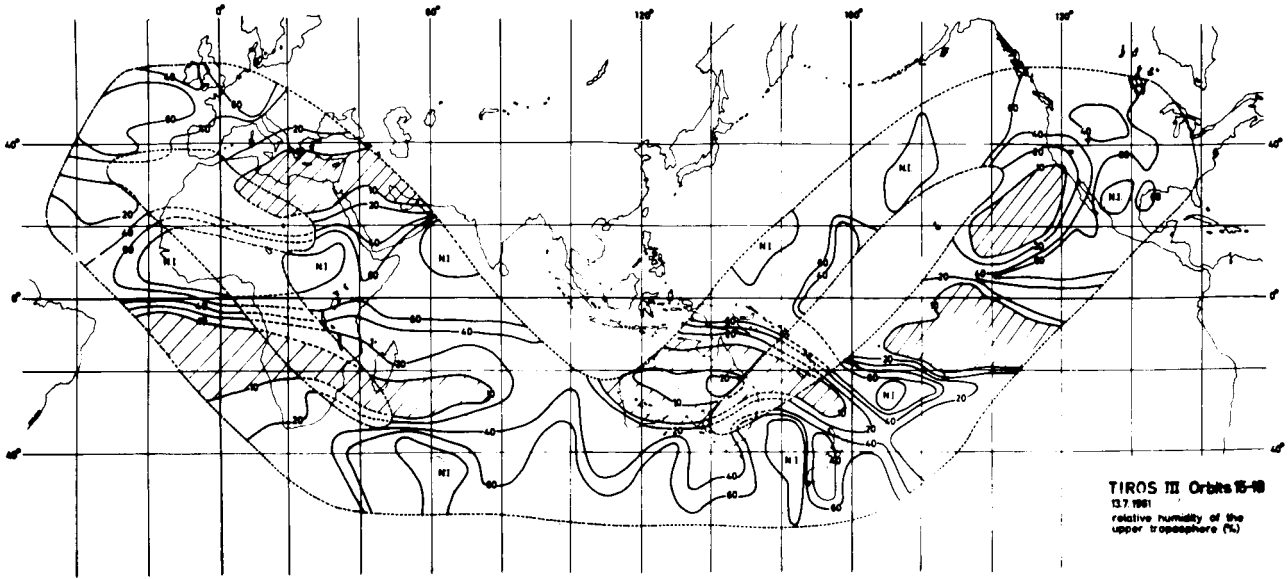
TIROS III Orbits 1-5
12.7.1961
relative humidity of the
upper troposphere (%)

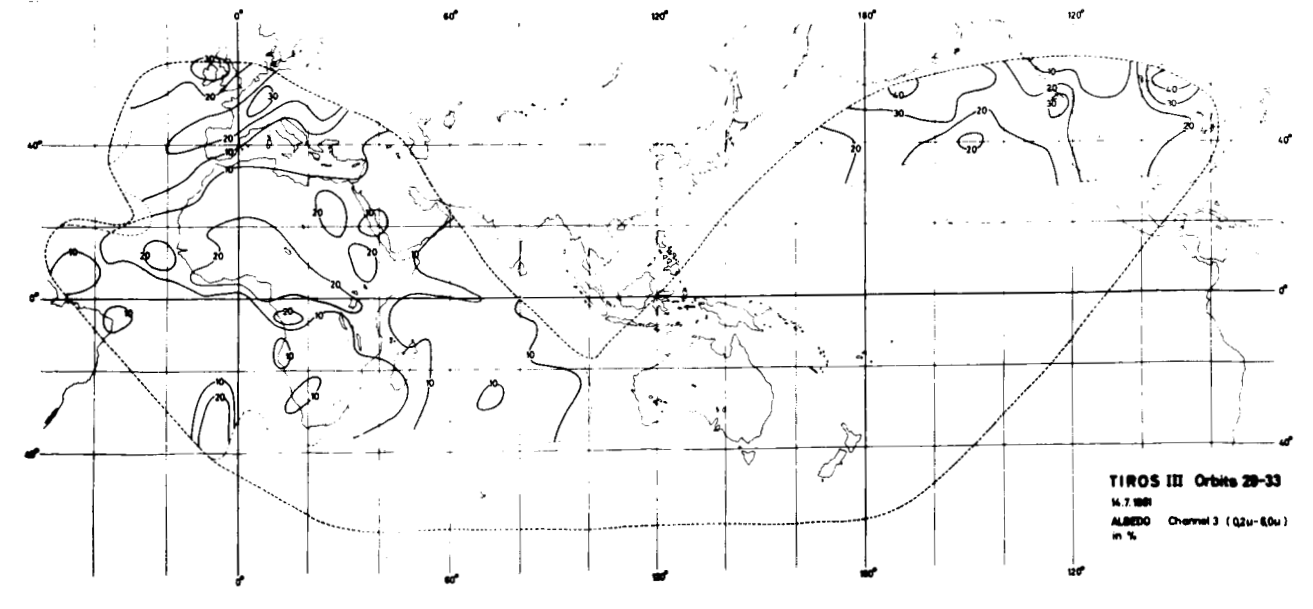
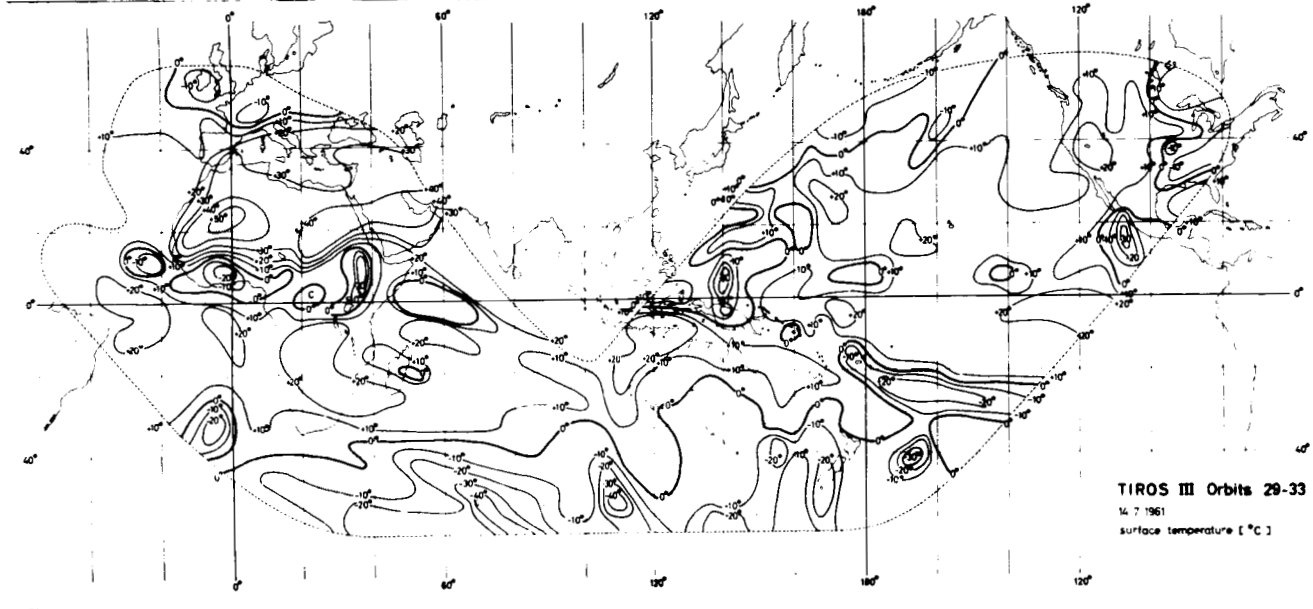
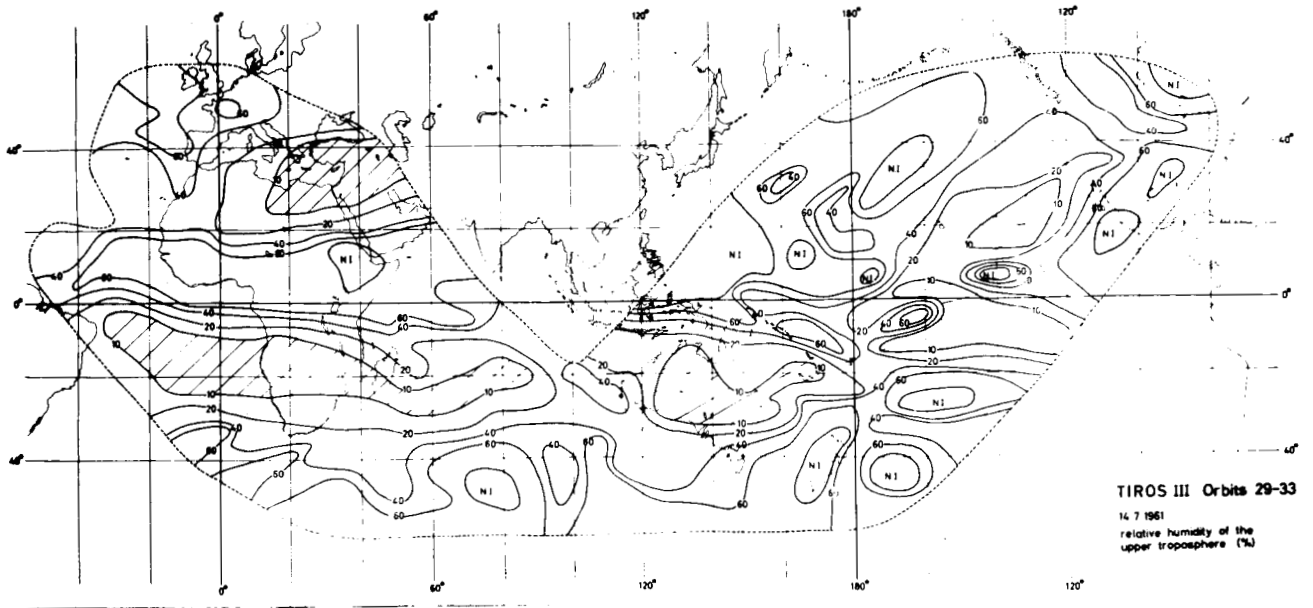


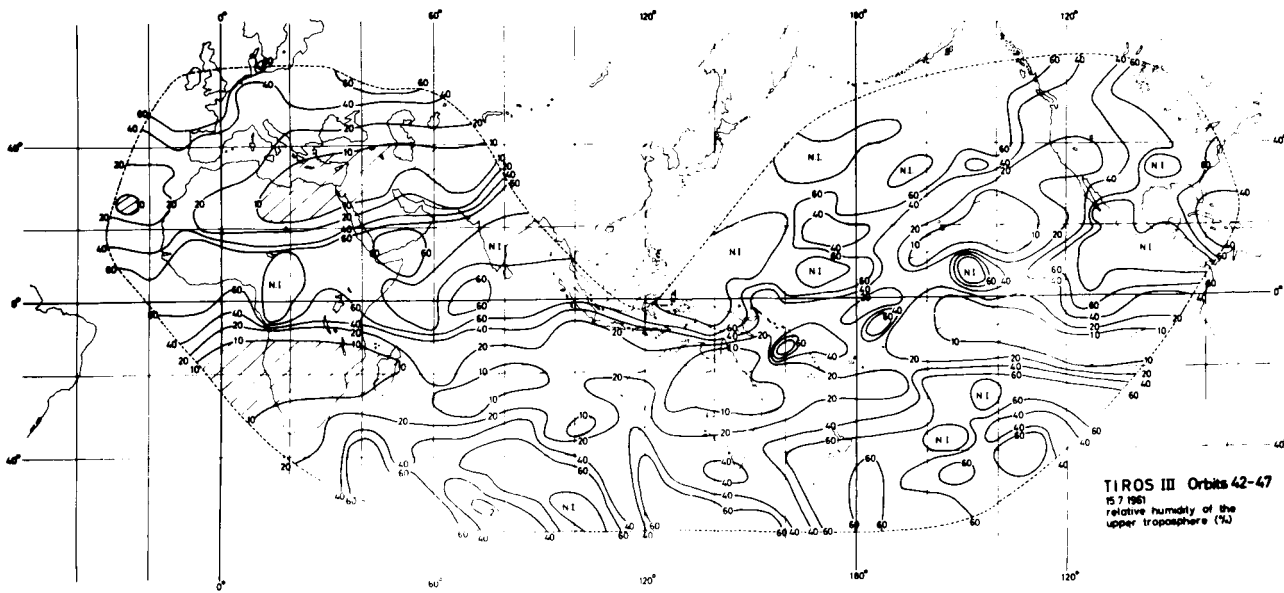
TIROS III Orbits 1-5
12.7.1961
surface temperature in °C



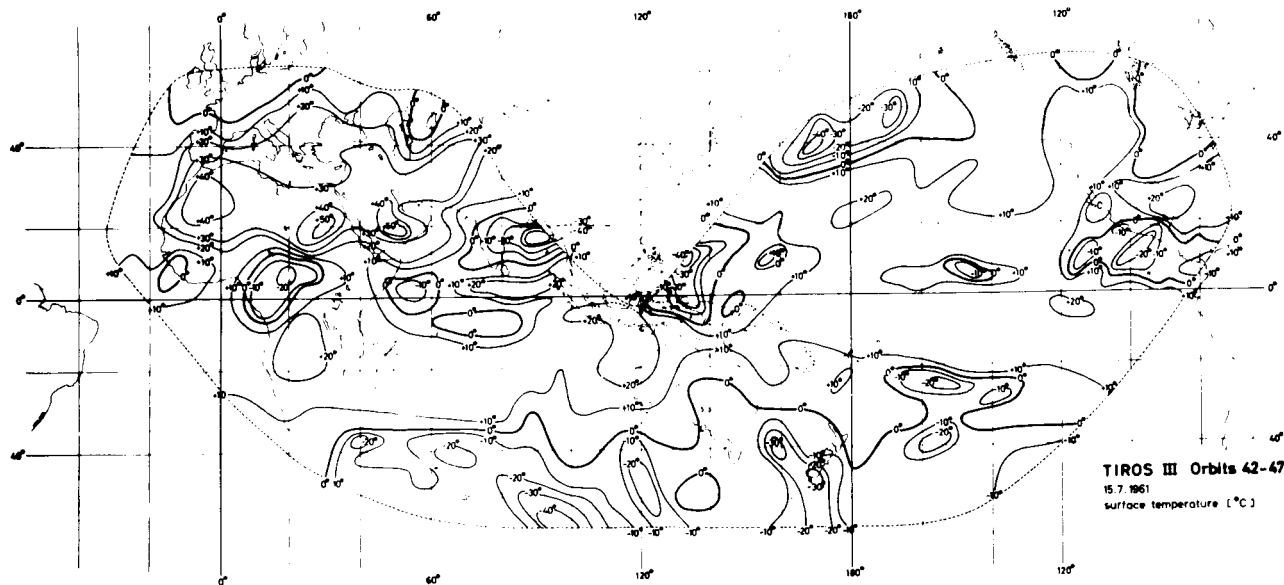
TIROS III Orbits 1-5
12.7.1961
ALBEDO Channel 3 (0.2-0.8µ)
in %



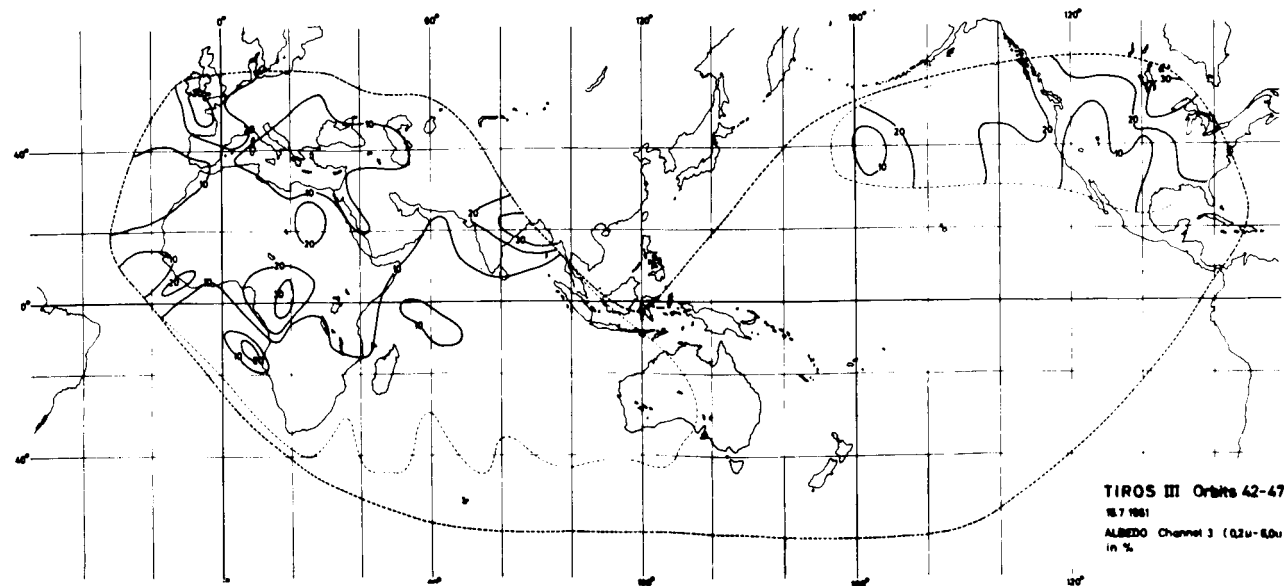




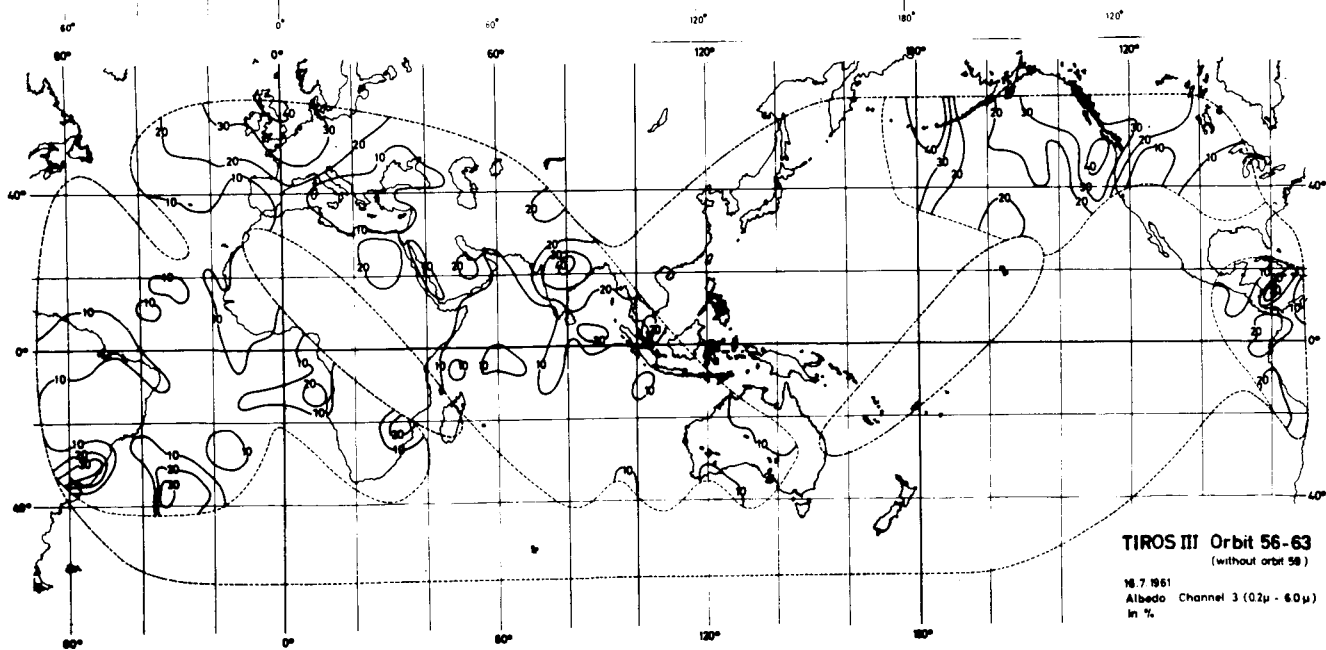
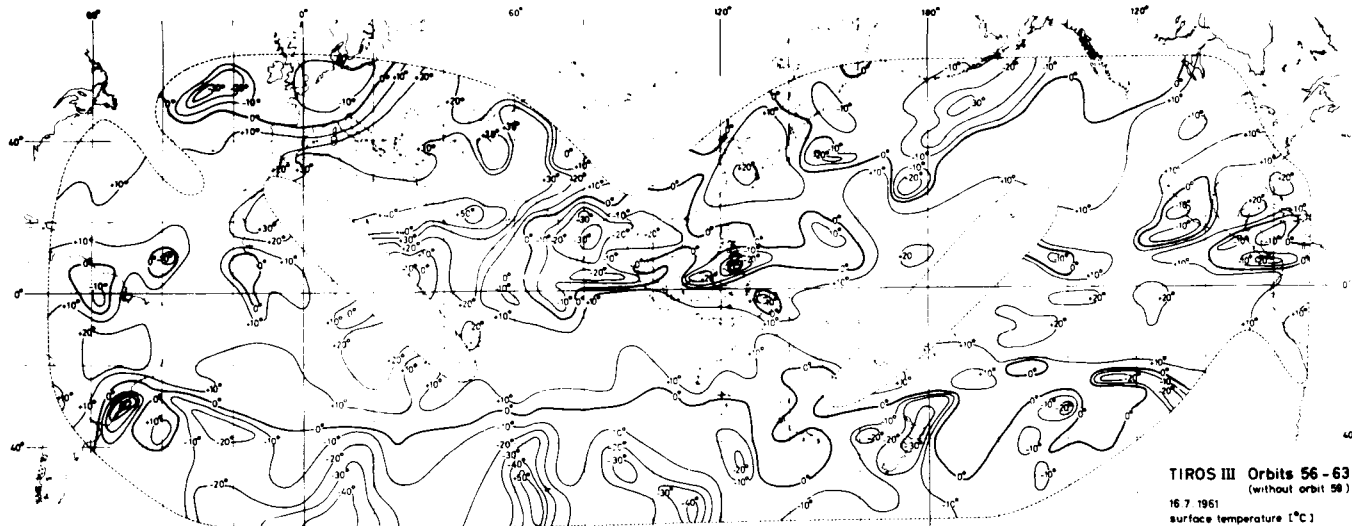
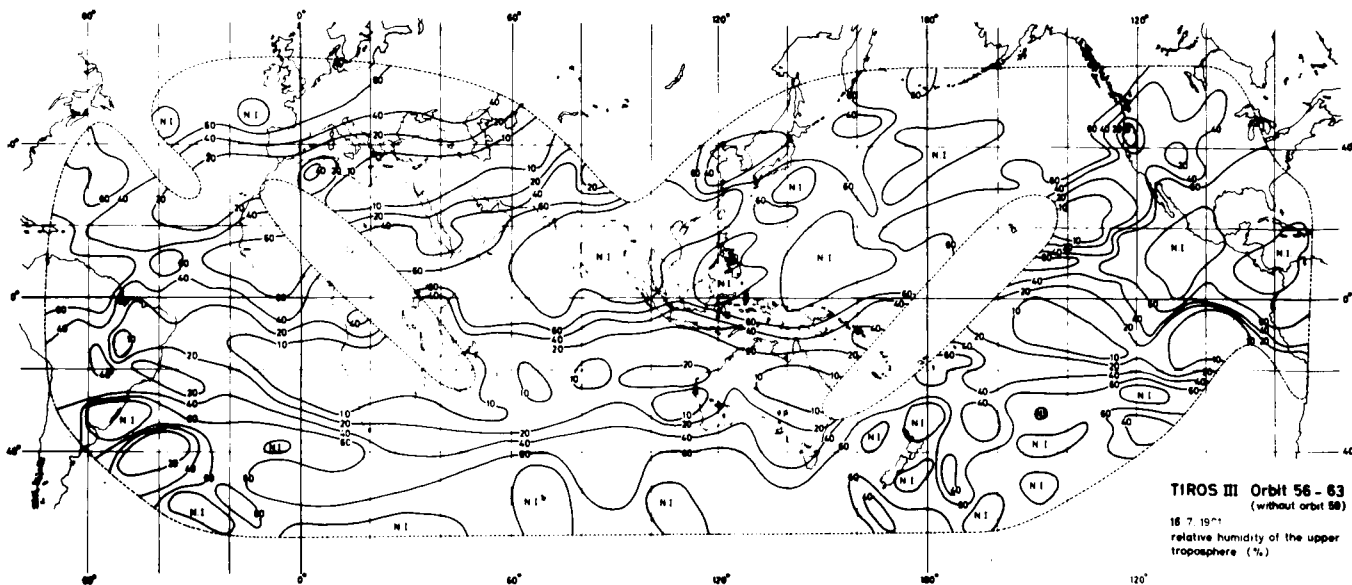
TIROS III Orbits 42-47
15.7.1961
relative humidity of the
upper troposphere (%)

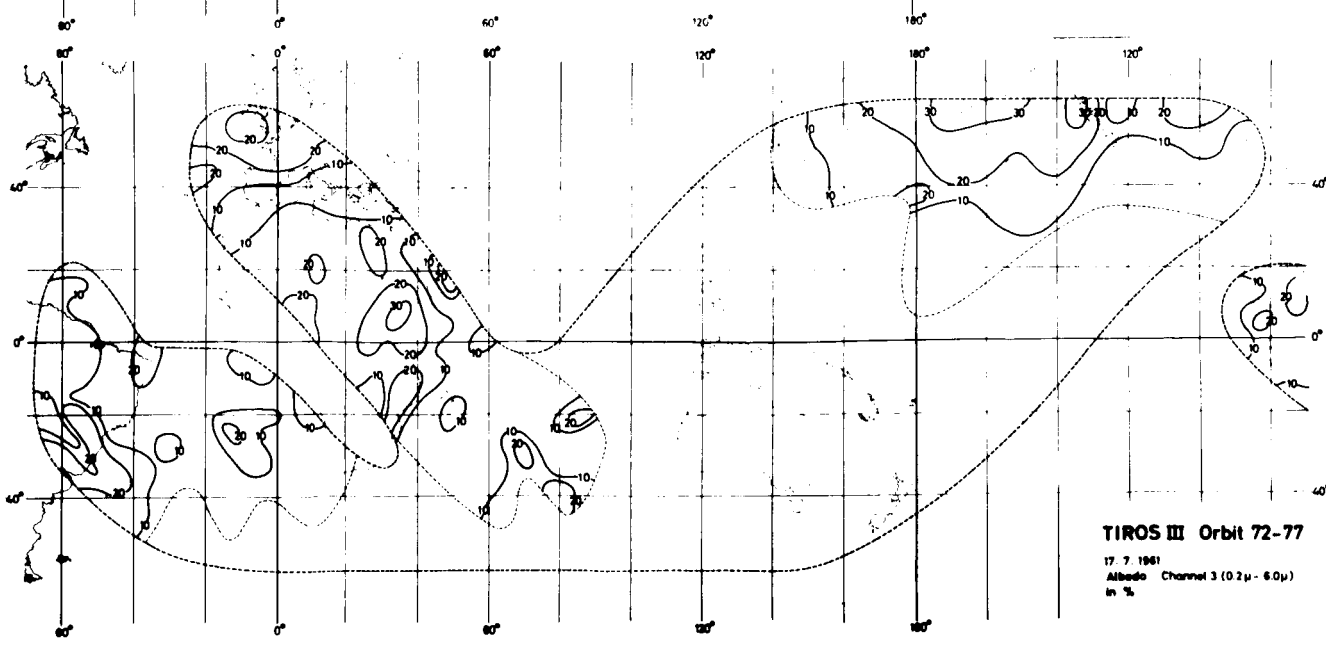
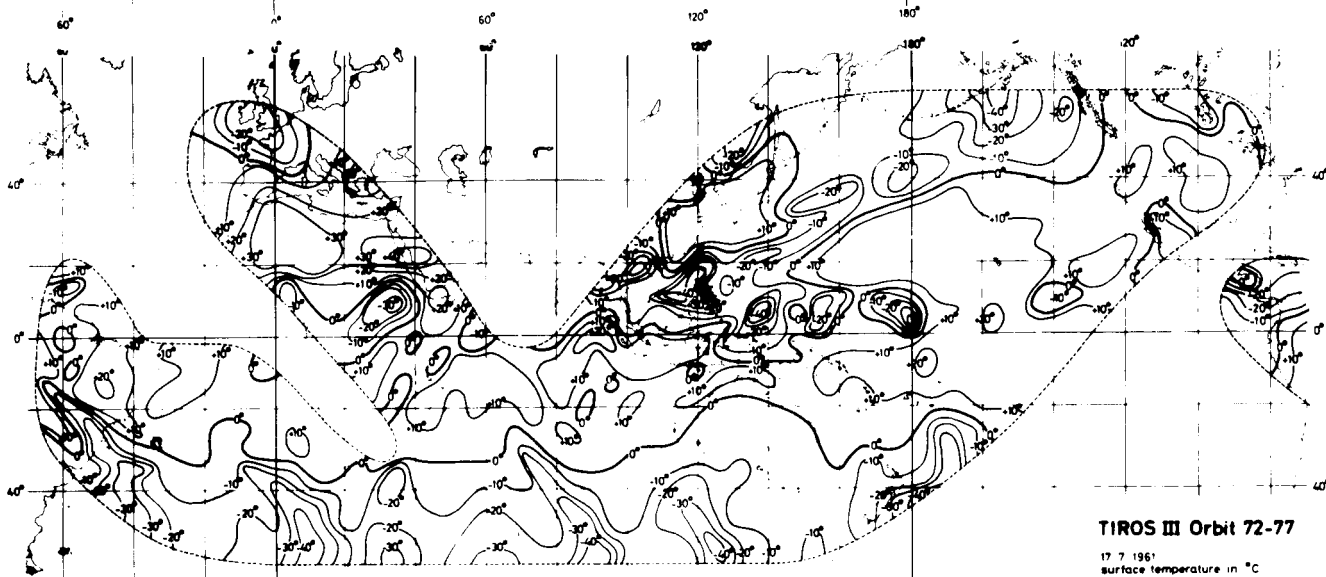
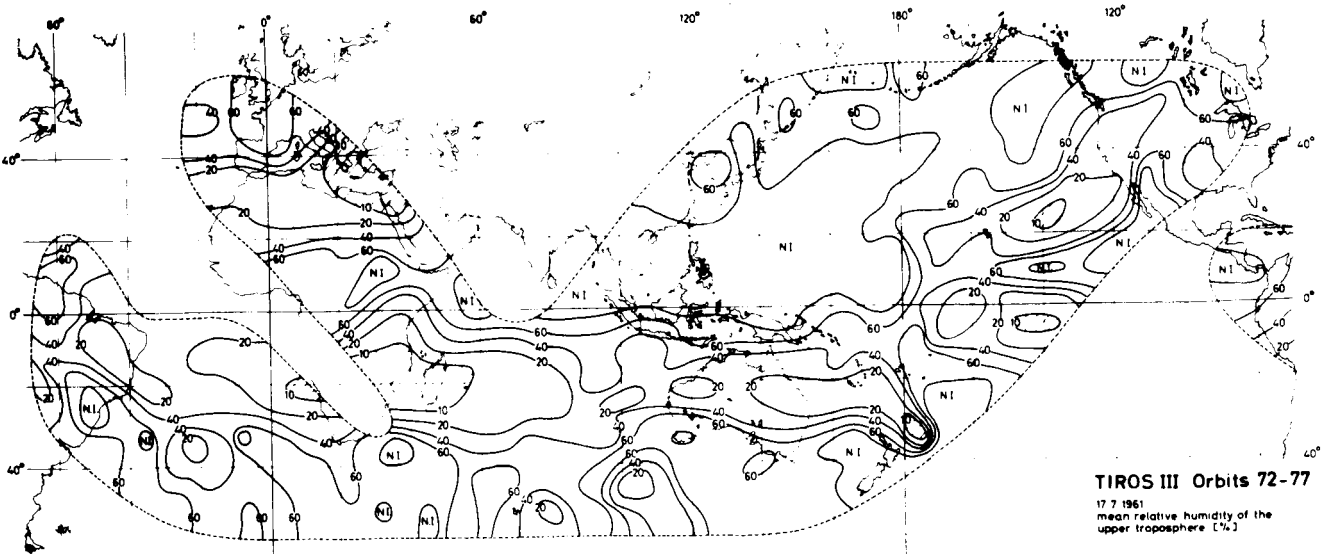


TIROS III Orbits 42-47
15.7.1961
surface temperature (°C)



TIROS III Orbits 42-47
15.7.1961
ALBEDO Channel 3 (0.2μ-0.6μ)
in %





determined. (The relative humidity of the upper troposphere in all areas designed by N. I. has been assumed to be 100 %).

This "meridional distribution (Fig. 19) of the mean relative humidity of the upper troposphere" shows low values at 28 degrees North (38 %) and 22 degrees South (16 %). The relative humidity over the Northern hemisphere is higher than over the Southern. This may depend on the selection of the orbits which do not cover all longitudes. Furthermore a very high cloudiness and high humidity usually occur over the Northwestern Pacific.

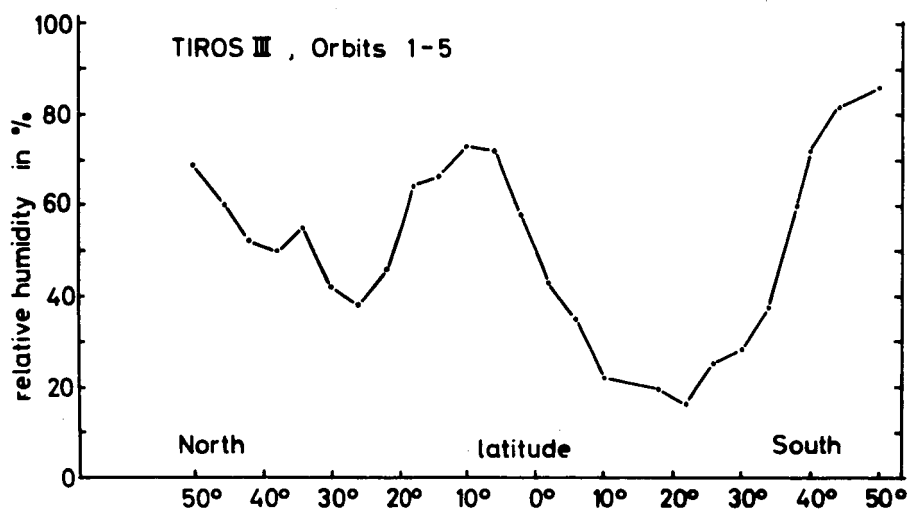


Fig. 19: Meridional distribution of the mean relative humidity of the upper troposphere, derived from radiation data from the orbits 1 - 5.

In the maps the areas with low surface temperature, corresponding to overcast sky with high reaching clouds, are mainly located near the meteorological equator (ITC) and at high latitudes (higher than 40 degrees North and South). Highest temperatures have been found over the desert areas of Arabia and North Africa (approximately local noon).

Since simultaneous measurements of the surface temperature have not been carried out, when TIROS III passed a cloudless region, direct verifications of the surface temperatures are not possible. Therefore only comparisons of the surface temperature over the open sea with the mean temperature of the water in July in the same region [12] have been possible. As it has been described in [2] and [1], the radiation data of orbits 15 and 18 yielded surface temperatures which were 1° - 2° lower than the water temperature, whereas those for orbit 61 were 8° - 9° lower than the water temperature. This large difference is certainly due to the degradation of the sensors [13]. Since the effect of degradation has not been taken into account at the evaluations, all values of the relative humidity and the surface temperature determined from radiation data of orbits 29 - 77 are too low.

The maps of albedo are shown here only for comparisons. All albedo values are low nearly by a factor of 2 or 3.

5. Concluding remarks:

Apart from inaccuracies, which are connected with the TIROS III radiation measurements, informative statements have been derived on the "global distribution" of the mean relative humidity of the upper troposphere and of the surface temperature, as it would be viewed from space. The resulting values of the humidity appear very reliable and its averaged meridional distribution does correspond to our conception of the climatic effects of the general circulation. Remaining inaccuracies may be caused by deviations of the actual stratification of the atmosphere from the used models. Therewith the lack of further information on the presence of thin and high clouds near the tropopause, and of the humidity and temperature (perhaps channel 1 of

TIROS VII) of the lower stratosphere may play a particular part. For a more detailed analysis of the radiation data, measurements with a higher accuracy and higher resolution as those of the HRIR of Nimbus I [14] are desirable.

The maps in Fig. 1 - 18 show distributions of the relative humidity and of the surface temperature only for a sequence of 6 days. Informations on seasonal variations of the geographical distribution of the relative humidity or of the surface temperature will be obtained from an evaluation of the radiation data of TIROS IV, which will be done in the near future.

R e f e r e n c e s

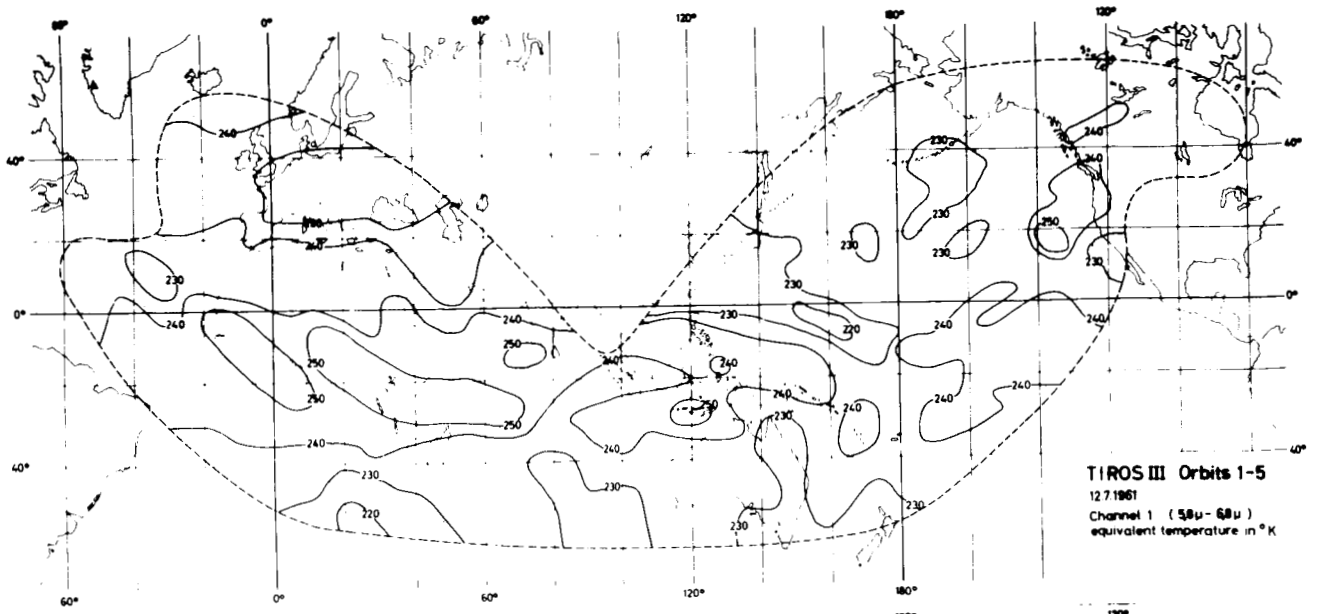
1. MÖLLER, F. and E. RASCHKE, (1964) : Evaluation of TIROS III Radiation Data, NASA CR - 112 , National Aeronautics and Space Administration, Washington , D.C.
2. RASCHKE, E. (1965) : Auswertungen von infraroten Strahlungsmessungen des meteorologischen Satelliten TIROS III , to be published in Beitr. Phys. Atm., Vol. 38.
3. RASCHKE, E. (1964) : Evaluations of TIROS III Radiation Data. Paper presented at the Symp. on Rad. Processes, Aug., 5. - Aug., 12. 1964 at Leningrad.
4. BANDEEN, W.R., M. HALEV, and I. STRANGE (1964) : A Radiation Climatology in the Visible and Infrared from the TIROS Meteorological Satellite. NASA TN - X 651 - 64 - 218, Paper presented at the Intern. Symp. on Rad. Processes, Aug., 5. - Aug., 12. 1961 in Leningrad.
5. ALLISON, L.J., J. I. GRAY, and G. WARNECKE (1964) : A Quasiglobal Presentation of TIROS III Radiation Data. NASA SP - 53, National Aeronautics and Space Administration, Washington, D.C.
6. TIROS III Radiation Data Users' Manual (1962) : Aeronomy and Meteorology Division of the Goddard Space Flight Center. National Aeronautics and Space Administration.
7. MÖLLER, F. (1961) : Atmospheric Water Vapor Measurements at 6 - 7 Microns From a Satellite. Planet. Space Sci. ., 5, 202 - 206.
8. WARK, D.Q., G. YAMAMOTO, and J.H. LIENESCH (1962) : Methods of Estimating Infrared Flux and Surface Temperature from Meteorological Satellites. J. Atm. Sci., 19, 369 - 384.
9. MÖLLER, F. (1962) : Einige vorläufige Auswertungen der Strahlungsmessungen von TIROS II. Arch. f. Met., Geoph., Biokl., Serie B, 12, 78 - 93.

10. PAETZOLD, H.K., and P. PISCALAR (1961) : Meridionale Ozonverteilung und stratosphärische Zirkulation.
Naturwiss., 48, 474.
11. GUTNICK, M. (1962) : Mean Annual Midlatitude Moisture Profiles to 31 km. AFCRL - 62 - 681, Air - Force - Surveys in Geoph. , No. 147.
12. U. S. NAVY, (1955, 1957, 1958) : Marine Climatic Atlas of the World.
13. BANDEEN, W.R., R. SAMUELSON, and I. STRANGE (1963) : TIROS III Radiation Data Users' Manual Supplement.
Aeron. and Met. Div., Goddard Space Flight Center, Greenbelt, Md.
14. NORDBERG, W., and H. PRESS (1964) : The NIMBUS I Meteorological Satellite.
Bull. Am. Met. Soc., 45, 684 - 687.

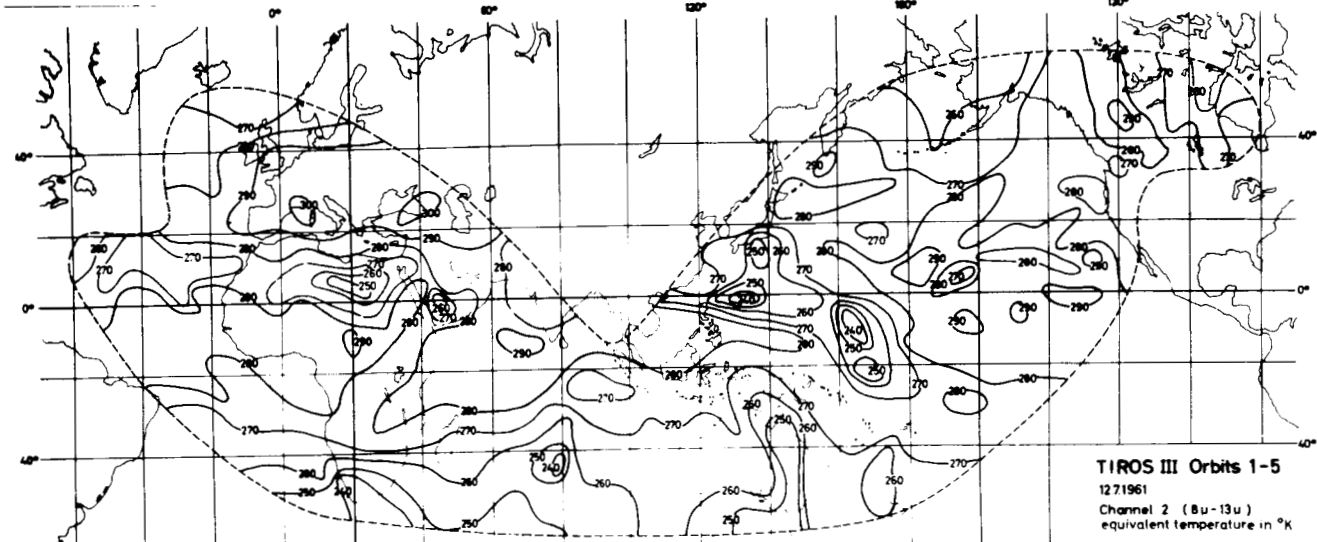
A p p e n d i x

Quasiglobal presentations of the TIROS III radiation data measured during the orbits 1 - 77 (July, 12 - July, 17 1961).

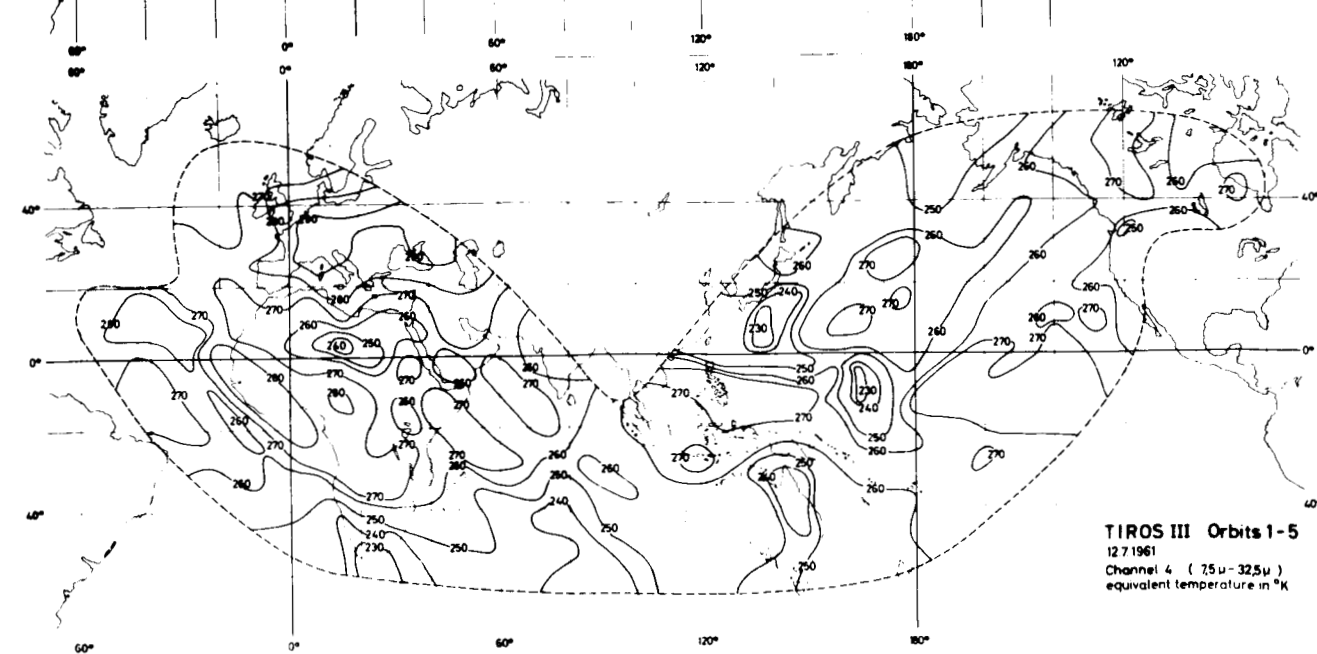
(By an error the geographic contour lines are shifted in the maps for the first 4 days 20 degrees southward.)



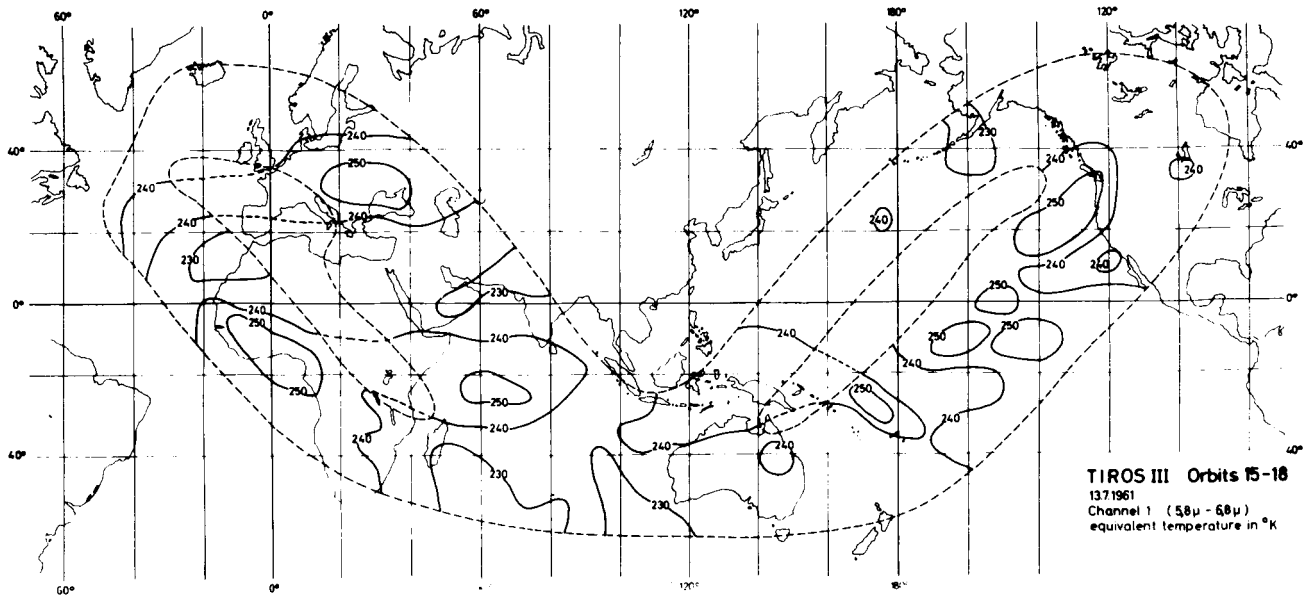
TIROS III Orbits 1-5
12.7.1961
Channel 1 (58u - 68u)
equivalent temperature in °K



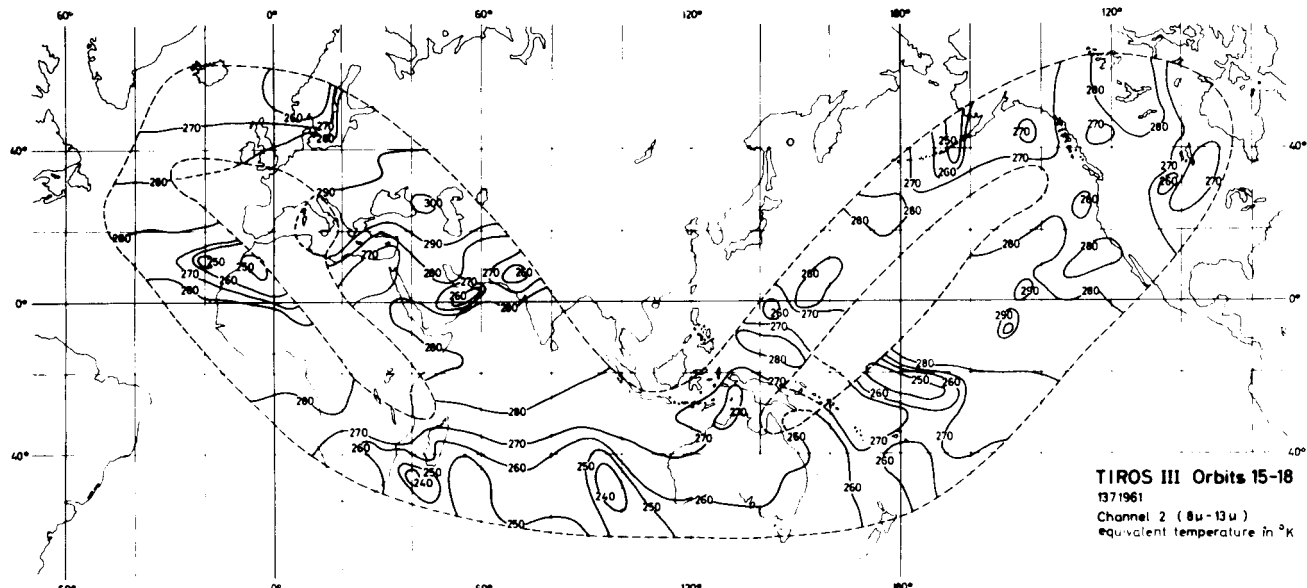
TIROS III Orbits 1-5
12.7.1961
Channel 2 (6u - 13u)
equivalent temperature in °K



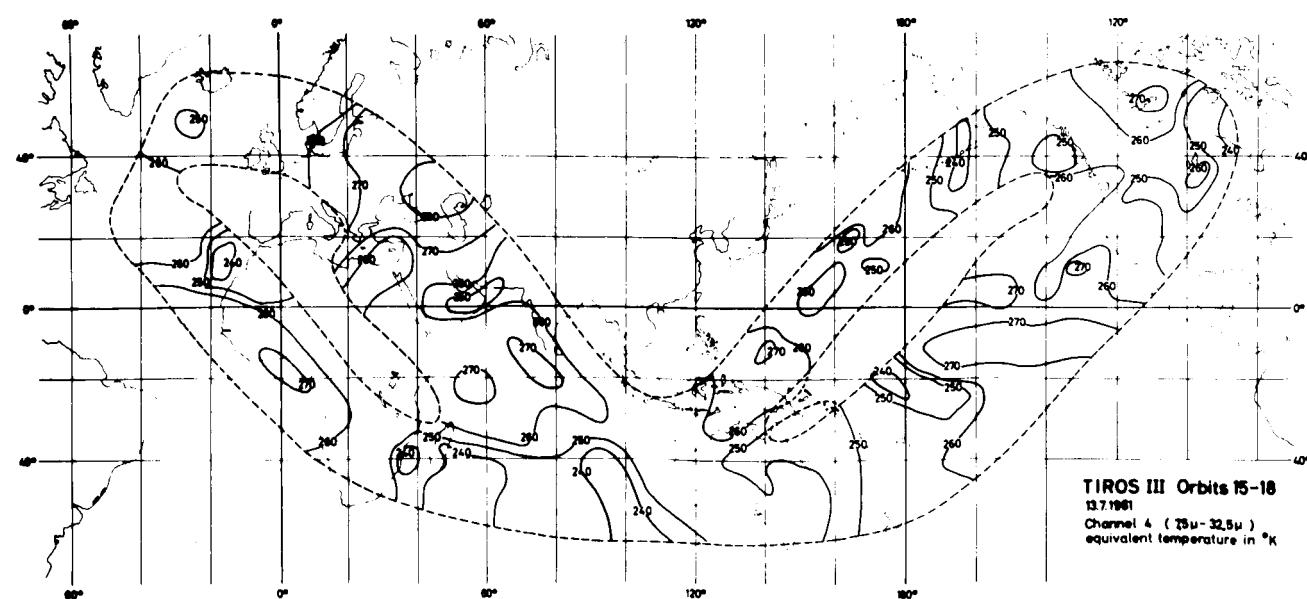
TIROS III Orbits 1-5
12.7.1961
Channel 4 (75u - 82.5u)
equivalent temperature in °K



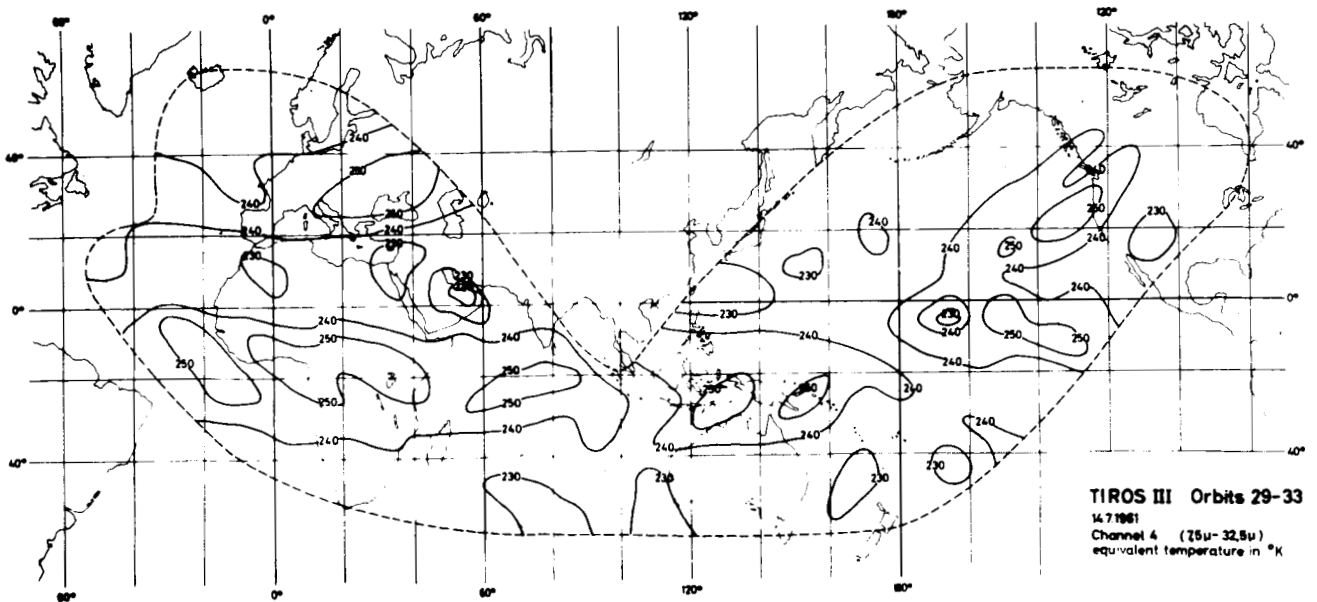
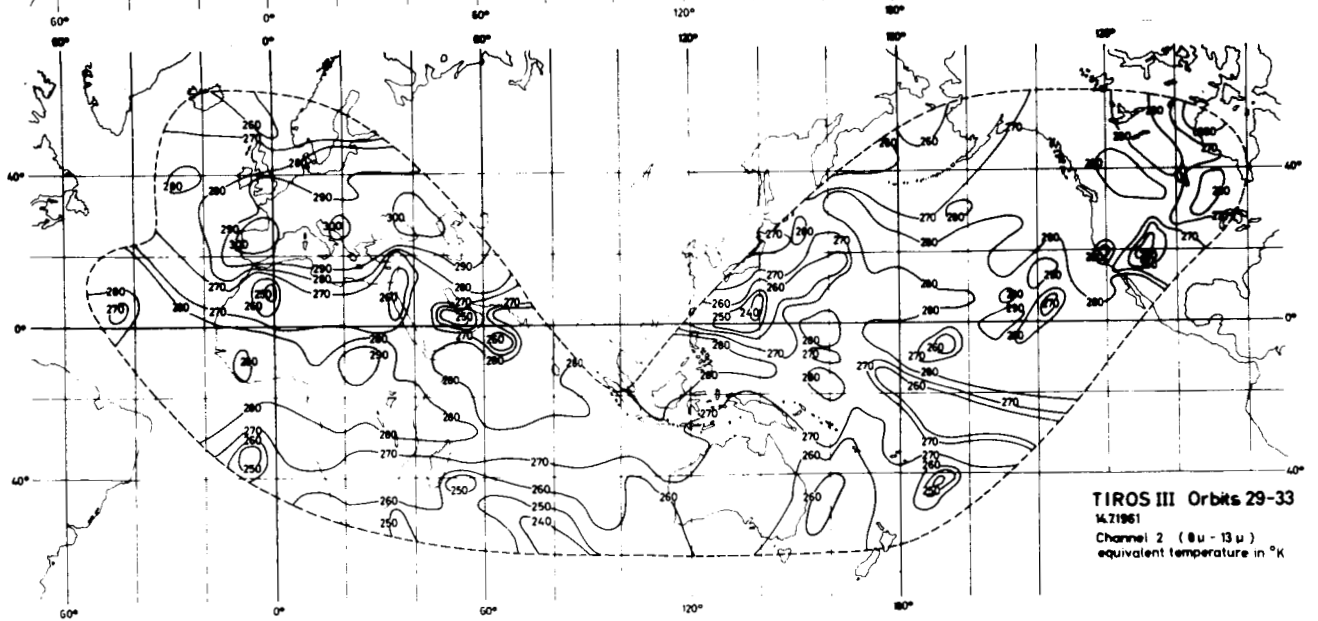
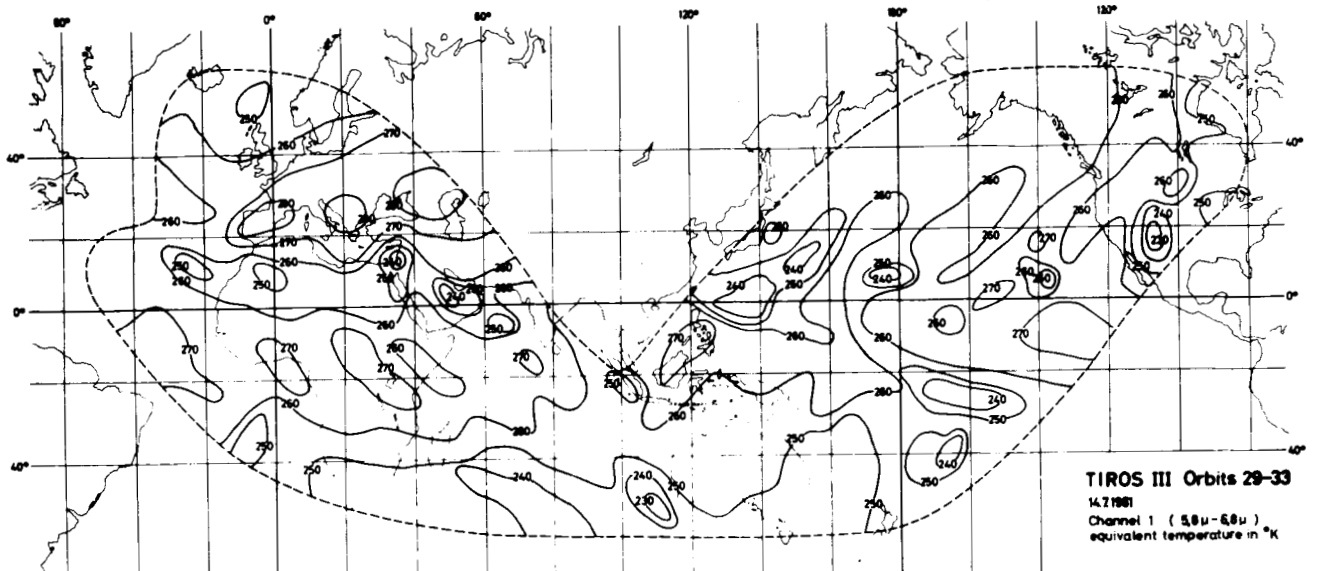
TIROS III Orbits 15-18
1371961
Channel 1 (5.8μ - 6.8μ)
equivalent temperature in °K

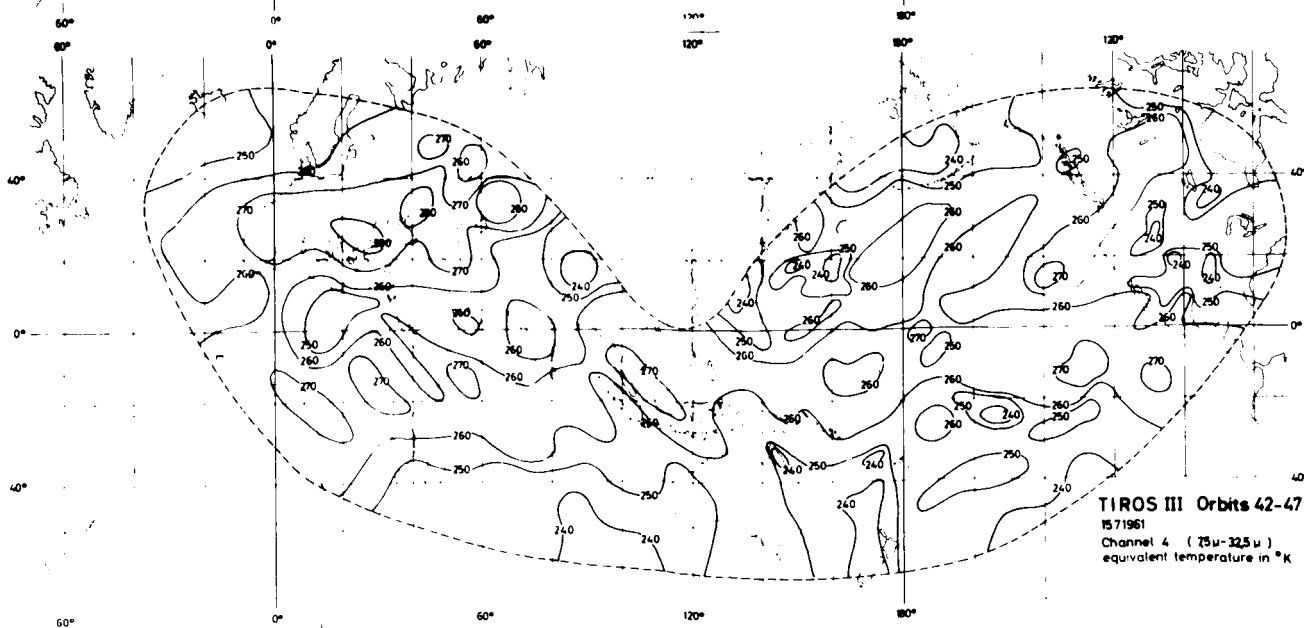
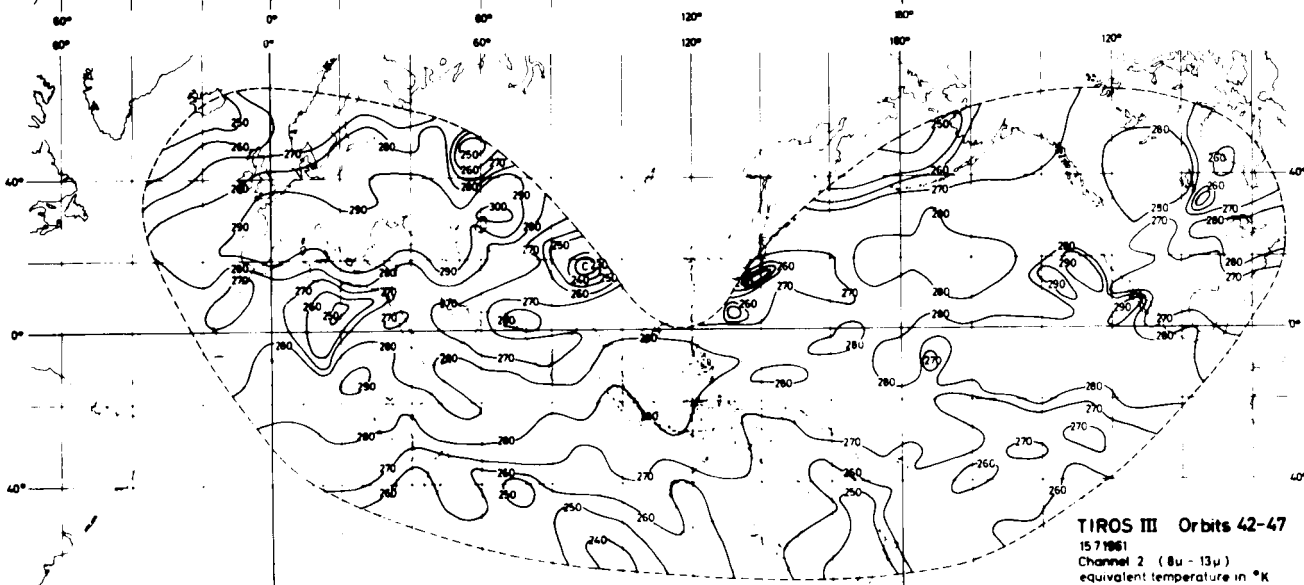
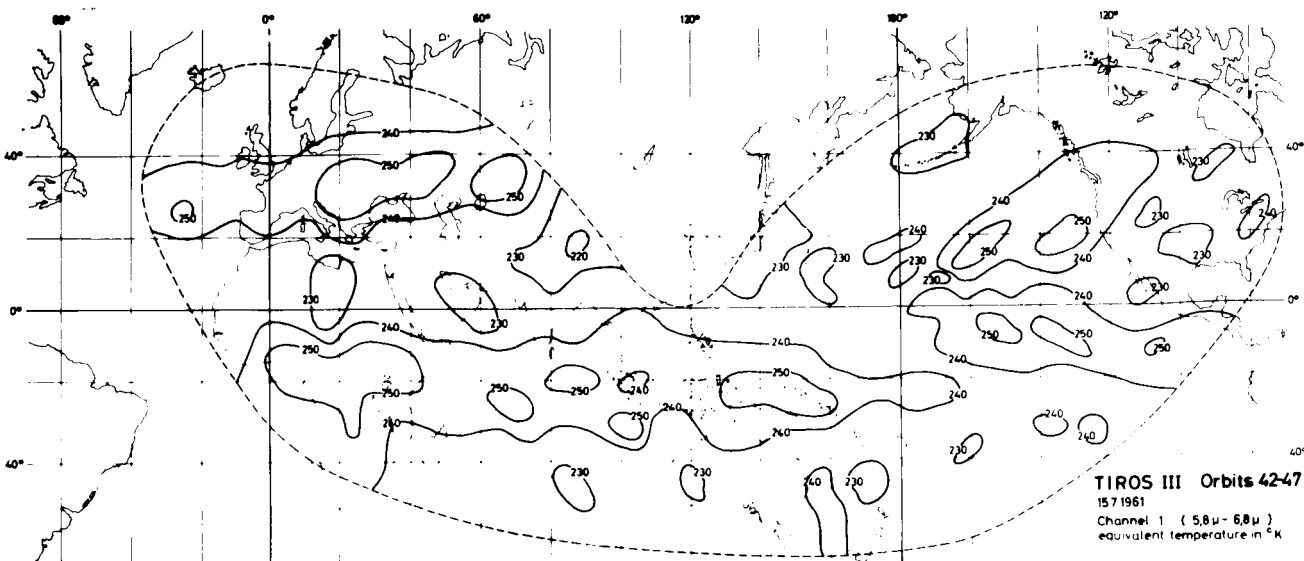


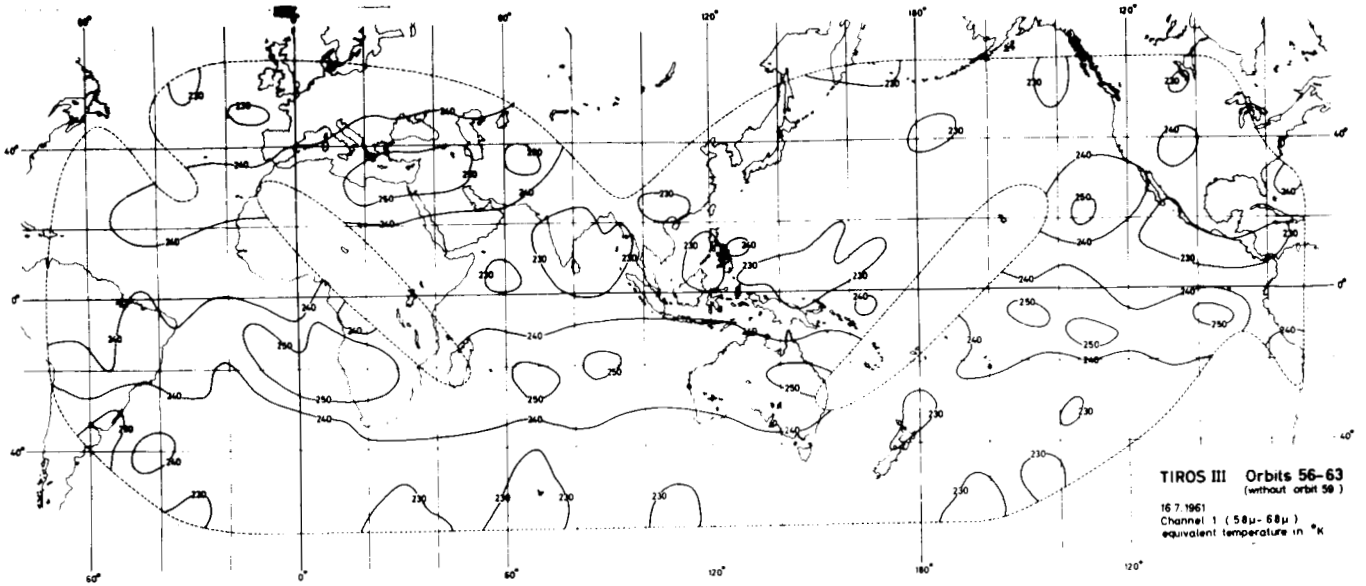
TIROS III Orbits 15-18
1371961
Channel 2 (8μ - 13μ)
equivalent temperature in °K



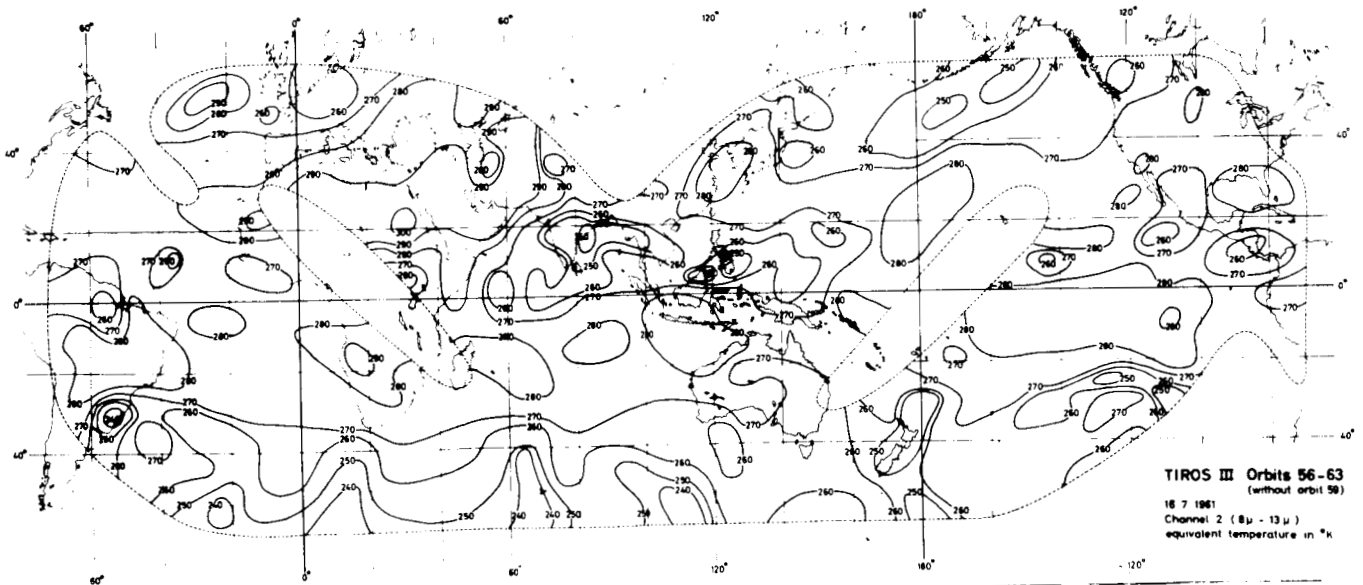
TIROS III Orbits 15-18
1371961
Channel 4 (25μ - 32.5μ)
equivalent temperature in °K



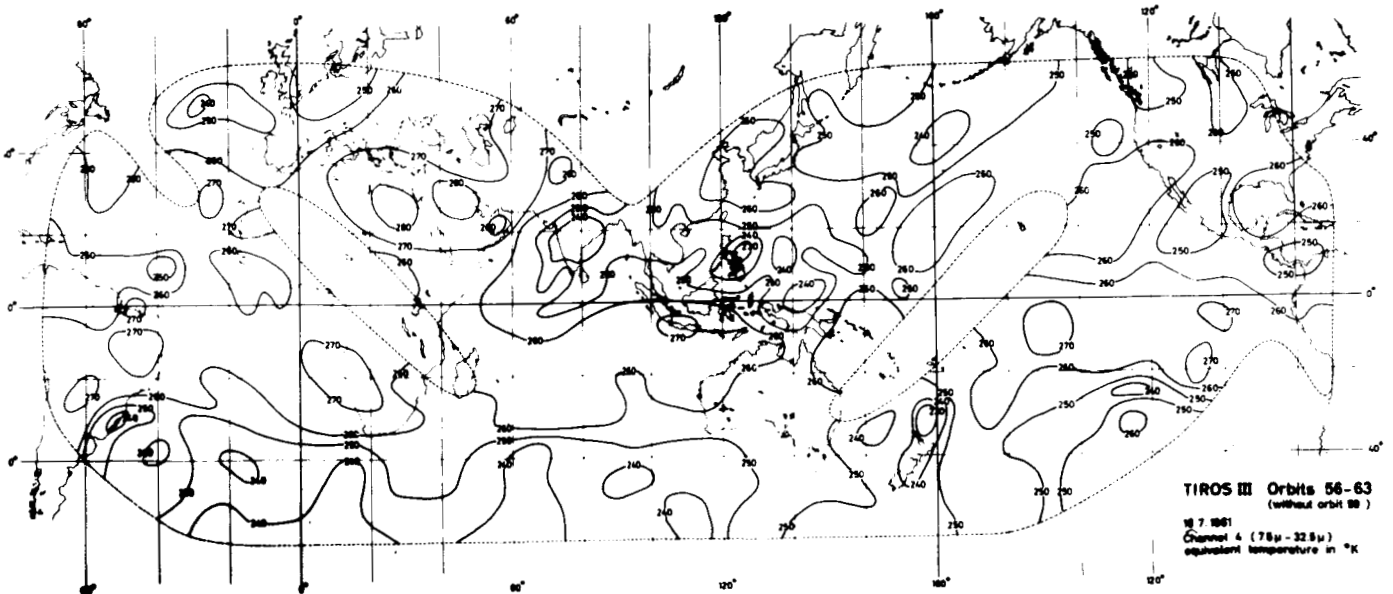




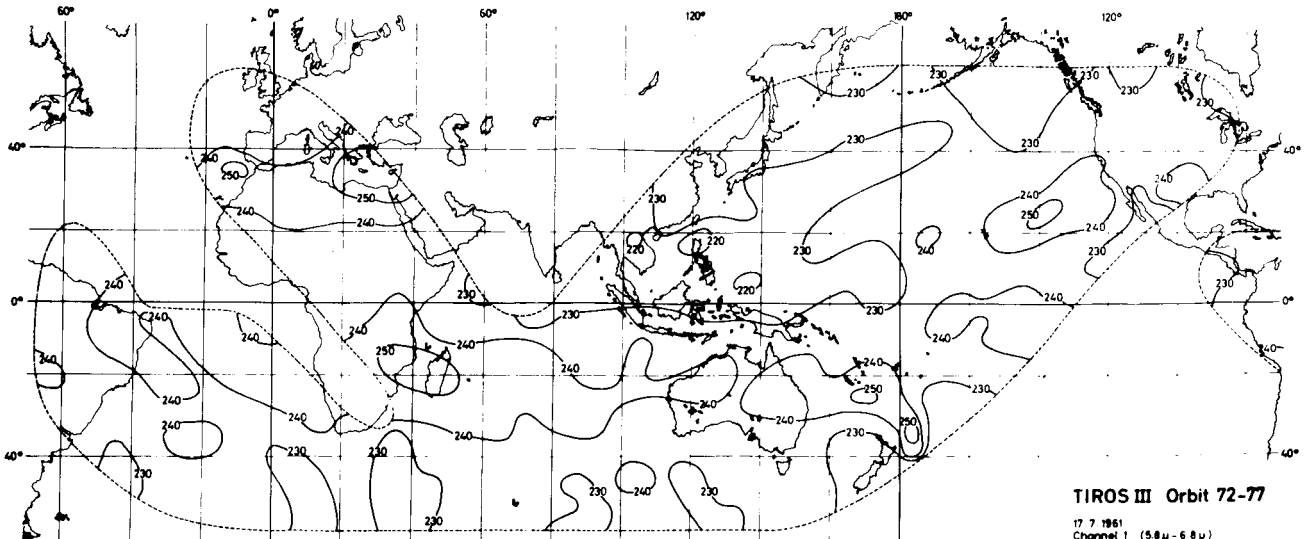
TIROS III Orbits 56-63
(without orbit 59)
16 7 1961
Channel 1 (58 μ - 68 μ)
equivalent temperature in $^{\circ}$ K



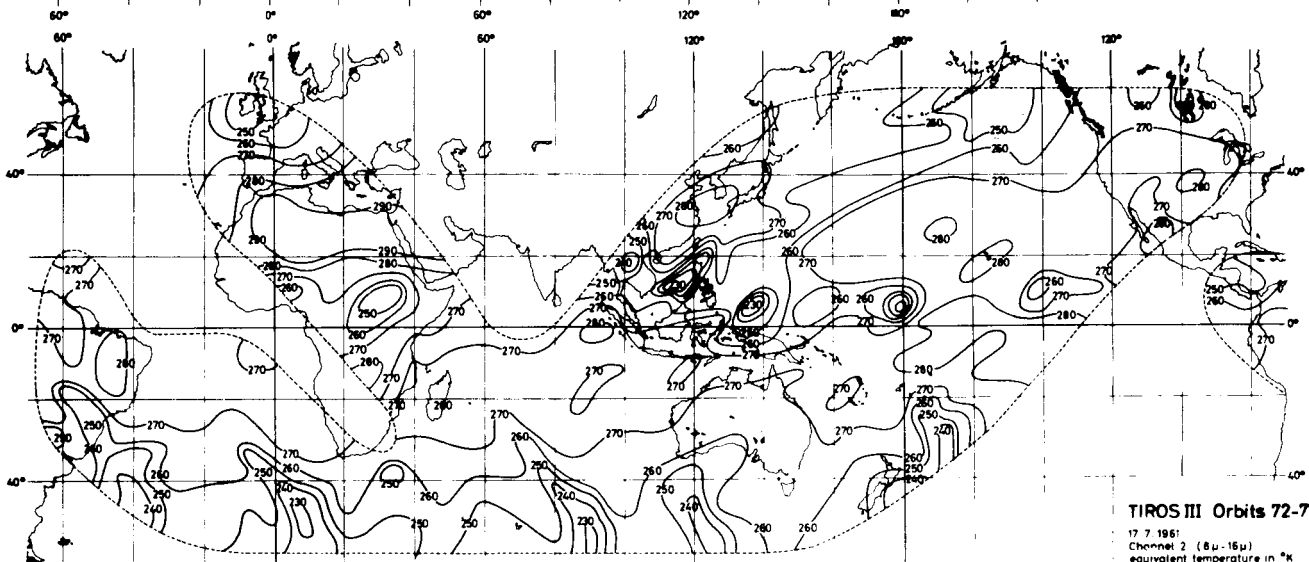
TIROS III Orbits 56-63
(without orbit 59)
16 7 1961
Channel 2 (8 μ - 13 μ)
equivalent temperature in $^{\circ}$ K



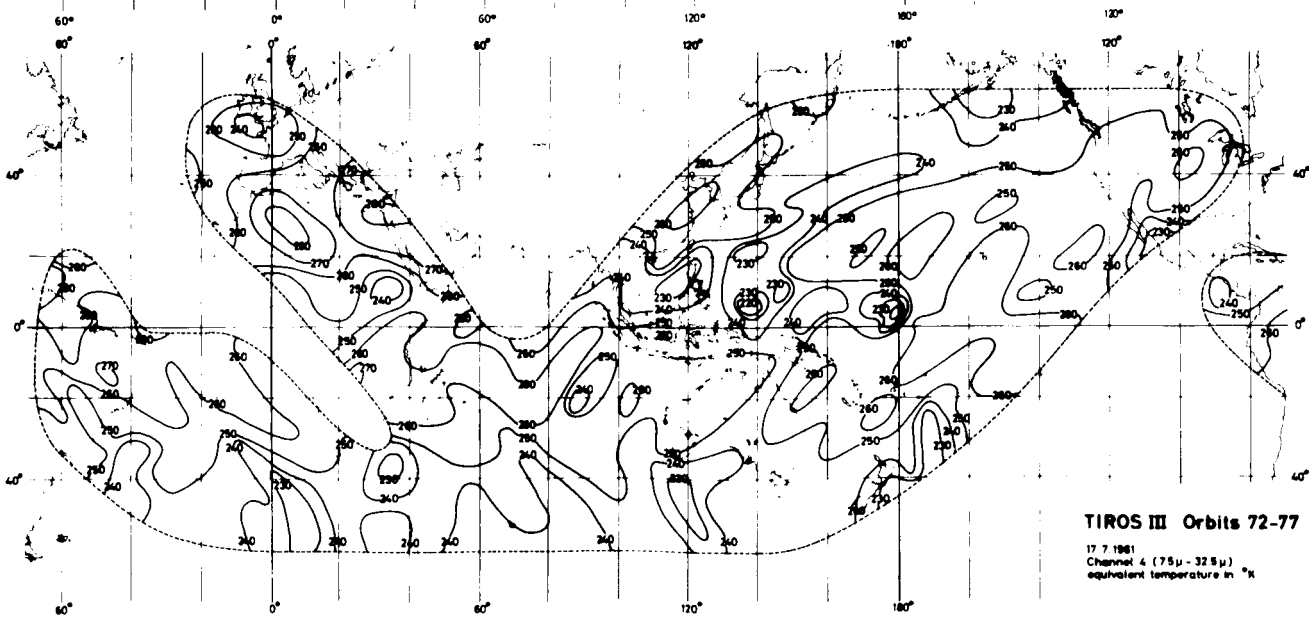
TIROS III Orbits 56-63
(without orbit 59)
16 7 1961
Channel 4 (7.8 μ - 12.8 μ)
equivalent temperature in $^{\circ}$ K



TIROS III Orbit 72-77
17.7.1961
Channel 1 (5.8 μ -6.8 μ)
equivalent temperature in °K



TIROS III Orbits 72-77
17.7.1961
Channel 2 (8 μ -16 μ)
equivalent temperature in °K



TIROS III Orbits 72-77
17.7.1961
Channel 4 (7.5 μ -32.8 μ)
equivalent temperature in °K

PART II

Influence of Minor Constituents
on the Outgoing Radiation

TABLE OF CONTENTS

List of figures	
List of tables	
Abstract	1
I. Introduction	2
II. The outgoing radiation: The equation of radiative transfer, its representation and inversion	4
a) Transmission function: representation and discussion	4
b) Application of the transmission function in smaller spectral regions (also in overlapping cases)	10
c) Planck function as term of the equation of radiative transfer	12
d) Vertical distribution of atmospheric gases and their influence on the upward directed radiation in the atmosphere	23
III. Results and conclusions	28
IV. References	36

LIST OF FIGURES.

Figure		Page
1	Transmission function τ for H_2O in the spectral range 2625-3225 (cm^{-1}) after Plass at different masses, pressures and temperatures	11
2	Transmission $\bar{\tau}^*$ of layers with growing thickness, starting from 10 mb to the earth surface. The influence of different gases is investigated. $\Delta\nu = 2030-2290$ (cm^{-1})	13
3a	Outgoing radiation F at 10 mb. The influence of the choice of ν_s (the frequency parameter in the Planck-function) is shown. $\Delta\nu = 2625-3225$ (cm^{-1})	15
3b	Influence of the choice of ν_s (the frequency parameter in the Planck-function) on the equivalent temperature $T_{\bar{a}}$ which is attached to the outgoing radiation. $\Delta\nu = 2625-3225$ (cm^{-1})	16
4	Equivalent temperature for the outgoing radiation at 10 mb. Absorber quantities are varied. $\Delta\nu = 2625-3225$ (cm^{-1})	20
5	Equivalent temperature for the outgoing radiation at 10 mb obtained by different ways of calculation. $\Delta\nu = 1210-1410$ (cm^{-1})	21
6	Equivalent temperature for the outgoing radiation at 10 mb. $\Delta\nu = 2030-2224$ (cm^{-1}).....	22
7	Equivalent temperature for the outgoing radiation at 10 mb. $\Delta\nu 2143-2290$ (cm^{-1})	22

Figure		Page
8	Equivalent temperature for the outgoing radiation at 10 mb. $\Delta\nu = 2030-2290 \text{ (cm}^{-1}\text{)}$	22
9	Outgoing radiation at 10 mb. Absorber quantities are varied	29
10	Equivalent temperature for the outgoing radiation at 10 mb. Absorber quantities are varied. $\Delta\nu = 1210-1410 \text{ (cm}^{-1}\text{)}$	30
11	Outgoing radiation at 10 mb. Absorber-quantities are varied. $\Delta\nu = 2030-2290 \text{ (cm}^{-1}\text{)}$	31
12	Equivalent temperatures for the outgoing radiation at 10 mb. Absorber quantities are varied. $\Delta\nu = 2030-2290 \text{ (cm}^{-1}\text{)}$	32
13	Outgoing radiation at 10 mb in relation to the case, when water vapor is the only absorber. Absorber quantities of N_2O and CH_4 are varied. $\Delta\nu = 1210 - 1410 \text{ (cm}^{-1}\text{)}$	33
14	Outgoing radiation when different atmospheric gases are regarded in relation to the case when only water vapor respectively water vapor and CO_2 are present. $\Delta\nu = 2030-2290 \text{ (cm}^{-1}\text{)}$	34
15	Outgoing radiation at 10 mb in relation to the case when water vapor is the only absorber. Absorber quantities are varied. $\Delta\nu = 2625-3225 \text{ (cm}^{-1}\text{)}$	35

LIST OF TABLES.

Table		Page
1	Example for cases, where the limits of validity of an empirical absorption function are not observed	9
2	Equivalent temperature from different sorts of calculation	24
3	Vertical distribution of water vapor	25
4	Mixing ratio and total content of atmospheric gases	26

ABSTRACT

The outgoing radiation is calculated in small spectral ranges, where the conditions become complicated as several atmospheric gases participate in absorption and emission.

A general computer program has been developed, which may be applied to any spectral range. Till now we have calculated in the following spectral regions (and in subdivisions)

- (1) 7.10 to 8.27 microns (1410 to 1210 cm^{-1})
- (2) 4.36 to 4.93 microns (2290 to 2030 cm^{-1})
- (3) 3.10 to 3.81 microns (3225 to 2625 cm^{-1})

where exist absorption bands of

- (1) H_2O , N_2O , CH_4
- (2) H_2O , CO_2 , N_2O , CO
- (3) H_2O , CH_4 .

The equivalent temperature differences caused by the neglect of the minor atmospheric constituents have been found to be in interval (1) about 8 degrees Kelvin, in interval (2) about 5 degrees Kelvin, in interval (3) about 2 degrees Kelvin. The errors of calculations of the outgoing radiation which arise from the absorption functions and from the procedure of calculation are discussed, and their influence on the equivalent blackbody temperatures. Similar calculations may be important for the measurements in the HRIR channel of the Nimbus satellite between 3.4 to 4.2 microns, which is mapping the nighttime cloud cover. Between 3.4 to 4.2 microns the gases CO_2 , CH_4 , N_2O are absorbing.

I. INTRODUCTION.

In recent years a number of papers have been published concerning the interpretation of radiation data received from the meteorological satellites (Ref. 1-16).

The experience with these data and additional theoretical investigations indicate that it is necessary to execute measurements and investigations in spectral regions which are smaller than those used in the first TIROS experiments. The reason is that there are wanted more detailed information about the vertical structure of the atmosphere, (for instance the vertical distribution of temperature and absorber concentrations) and about radiation processes (for instance radiative heating and cooling). Theoretical investigations have been made for instance by Kaplan, King, Wark, Yamamoto, Smith, and others (Ref. 16-29), especially for the infrared part of the electromagnetic spectrum, but also for the microwave part.

The first practical method to derive a meteorological parameter from TIROS satellite measurements has been proposed by Möller (1960) and developed in references 6, 19. By his method it is possible to deduce the relative humidity of the upper troposphere and the surface temperature of the Earth respectively of clouds. These investigations were the starting point for extensive interpretations of TIROS-radiation measurements.

Meanwhile the instruments have been further developed and it is possible to make radiation measurements from satellites in spectral intervals, which are essentially smaller than the TIROS-channels. For instance the Nimbus Weather Satellite has a high resolution infrared radiometer (HRIR) which measures the outgoing radiation between 3.4 and 4.2 microns. It maps the nighttime cloud cover by measuring the energy received in this spectral region. It is very valuable to get this nighttime weather information.

It is the purpose of our investigation to make possible a correct interpretation of radiation data in smaller spectral regions. Therefore, we calculate the possible errors introduced into the evaluation of outgoing radiation measurements by too rough approximations in the equation of radiative transfer. It is necessary to have a precise knowledge of each parameter entering the equation of radiative transfer. Therefore, we will discuss the influence of these parameters and their approximations. Especially it is necessary to have good knowledge of the transmission functions as functions of pressure, absorber mass and temperature. One needs these functions for the range of values which may adopt their parameters in the Earth atmosphere. If different gases are absorbing in one spectral interval it is necessary to regard the influence of the overlapping of their absorption bands on the outgoing radiation. The transmission functions of the single gases must be multiplied.

In the present report we calculate the outgoing radiation in regions where the conditions are complicated because of the presence of several absorbing gases. For our calculations we use experimental absorption functions, and where such are lacking, theoretical calculation. The method is general and can be applied to any spectral region and to any absorbing gas, if the transmission functions and the vertical distribution of the gases are known. The number of gases, possible to be regarded, is not restricted.

II. THE OUTGOING RADIATION: THE EQUATION OF RADIATIVE TRANSFER, ITS REPRESENTATION AND INVERSION.

The equation of radiative transfer is:

$$[1] F_{\Delta\nu}(U, \theta) = \int_u^\infty B_{\Delta\nu}(T_0) d\tau(U \sec \theta) + \int_0^u B_{\Delta\nu}[T(z)] d\tau_{\Delta\nu}[(U-u) \sec \theta]$$

where

$\Delta\nu$ frequency interval in wavenumbers

$F_{\Delta\nu}$ outgoing radiation in the interval $\Delta\nu$
departing from the upper boundary of the atmosphere

$T(z)$ temperature as a function of z

T_0 ground temperature

z height

$B_{\Delta\nu}$ Planck's function in the frequency range

$\tau_{\Delta\nu}$ transmission function of the atmosphere in the
frequency range $\Delta\nu$

θ nadir angle of the direction of observation

u effective mass of the absorbing substance

U total mass of the absorbing substance.

The parameters of Eq. [1] are essential for the influence on the outgoing radiation for the interpretation of satellite radiation measurements. As consequence we discuss in the following these parameters and the influence of their variation on the outgoing radiation and on the related equivalent temperature. As these parameters influence the outgoing radiation, their errors cause uncertainties in the deduction of the vertical structure of the atmosphere, that means in inversion processes.

II. a) Transmission functions: representation and discussion.

For the representation of the absorption of atmospheric molecular bands there are known four methods:

- (1) Theoretical summation over the contributions of all lines forming the band. For this procedure it is neces-

sary to know the line-parameters deducible from the quantum mechanics of rotation and vibration transitions: position, strength, halfwidth. It is usual to take models and assumptions or approximations for line shape (for instance Lorentz-shape, combined Lorentz-Doppler shape, Doppler-shape), pressure dependence and temperature dependence, for instance

$$[2] \quad \frac{\alpha_L}{\alpha_0} = \frac{p}{p_0} \left(\frac{T_0}{T} \right)^{1/2}$$

where α_L = Lorentz-shape
 α_0 = halfwidth at NTP.

As it is impossible to regard all lines together by the summing up of their contributions, one must eliminate the weak lines. This can be a source of errors (Ref. 44).

- (2) Theoretical calculation with the use of band models. One regards quantum mechanical data of strength, and position of lines in the band. Then one chooses an appropriate band model with mean values of line strength, halfwidth and distance of the lines. Assumptions and approximations are made for line shape and temperature dependence.
- (3) Deduction of the absorption from experimental data. The accuracy is given by the limits of the measuring device, for instance by the spectral resolution. As these empirical relations have always restricted regions of validity, it is sometimes difficult to use them in atmospheric problems, especially when the absorption band is weak and the used atmospheric layer thickness is small.
- (4) Fitting of experimental absorption data to theoretical band models; at this procedure it is difficult to regard the weak lines adequately.

To calculate the transmission of band models over inhomogeneous paths, Curtis and Godson (Ref. 34, 35, 36) have proposed their well known approximation (Ref. 45), where they introduce

a mean value of the halfwidth

$$[3] \quad \alpha = \frac{\int S \alpha dm}{\int S dm}$$

Already Kaplan (Ref. 37) has shown qualitatively and quantitatively that the application of this approximation to lines with Lorentz-shape leads to an overestimation of the absorption of inhomogeneous layers, especially at smaller pressures. Drayson (Ref. 28) has shown this too for the example of the 15 μ CO₂-band and has extended those consideration to paths with arbitrary pressure levels. The completest transmission data for H₂O and CO₂ have been given by Stull, Wyatt, and Plass (Ref. 38). In the recent time some authors have compared experimental measurements in the free atmosphere with calculation based on these tables:

- (1) Roney (Ref. 39) has measured solar spectra in the 2 to 5 micron region for atmospheric slant paths at heights of about 42.000 ft. He finds that his measurements show a much lower absorption than would be expected by the calculation based on the Plass-tables. He tries to explain the discrepancy with the Lorentz-line shape used by Plass and with effects due to refraction neglected by Plass. From Roney's spectra one may also recognize that the "Plass-spectra" are shifted in the direction of small wavenumbers compared with the measurements.
- (2) Measurements of the University of Denver (Ref. 48) show spectra obtained by means of a balloon borne spectrometer system in different heights. They compare their measurements with calculations basing on the Plass-tables, and they find: region 2100 to 2500: "if one shifts the observed spectra 9 cm⁻¹ (towards small wavenumbers) which is less than the uncertainty in the scale in this region, one notes that the spectra are in reasonably good agreement considering that the experimental results are due to

a combination of absorption by N_2O and CO_2 whereas the theoretical results are based on CO_2 only", region 1400 to 1800 cm^{-1} : "...the observed absorptions are less than predicted at all wavenumbers in spite of the fact that the observations were made 2.5 km below the altitude used in the theoretical spectrum. There is good agreement between the theoretical and experimental results as far as the position of the peak absorptions are concerned, but the relative strength of the individual absorptions are considerably different".

- (3) S.R. Drayson (Ref. 28) shows by means of theoretical calculations that the Plass-tables are not correct in the 15 micron region mainly for the following reasons:
- (a) "Plass was forced to use the Curtis - Godson approximation which tends to overestimate the absorption".
 - (b) "The line strengths (used by Plass) were not in perfect agreement".
 - (c) "Probably the greatest single cause is the use of the quasi-random band model".

From Drayson's calculations (Ref. 28, Fig. 8) one could observe that a shifting of Drayson's spectra towards smaller wavenumbers sometimes would give a better (but not full) agreement with Plass's results.

- (4) List and Oppel (Ref. 40) have used the Plass-tables for water vapor in the 4-5 micron region. For wavelengths larger than 4.5 microns, where H_2O is the dominant absorber, they find a difference between calculations and measurements; they suppose the reason for the discrepancy are the theoretical calculations (Plass) for the transmission of H_2O which they have used. A discrepancy in position between calculated and measured values can be observed too: the observed spectra must be shifted in direction of smaller wavenumbers to get a better agreement with the calculations. From the spectra one can deduce: $A_{\text{calculated}} > A_{\text{observed}}$ in most of the cases.

(5) Bolle (Ref. 41) has compared the transmission data in the region of 4.7 microns given by Taylor and Yates (Ref. 42) with those from Plass and has found that the latter are everywhere smaller than the premier. Bolle and Völker (unpublished) find from measurements of the spectral sky emission on the earth surface in the spectral range from 4.6 to 5.1 microns and 7.41 to 8.70 microns that there are essential discrepancies compared with the radiation to be expected by the Plass-tables.

For the absorption of atmospheric minor constituents Burch and al. (Ref. 31) give experimental absorption functions in dependence of pressure and absorber mass. They give empirical relations which mostly are written either in the form

$$[4] \quad A = \int A(\nu) \cdot d\nu = c[w \cdot P_e^a]$$

or

$$[4a] \quad A = \int A(\nu) d\nu = C + D \cdot \log[w \cdot P_e^a]$$

where a, b, c, C, D, are empirical constants, and c is approximately equal to 0.5;

P_e = equivalent pressure of the absorbing gas

w = absorber-mass

A = integrated absorption

ν = wavenumber.

It can be seen from [4], [4a] that a change of absorber mass must change the integrated absorption. If one uses these relations, of course one has to consider their limits of validity, but weak excess of these limits doesn't cause severe errors in the calculation of the outgoing radiation: see table 1, cases γ, δ . A strong excess causes greater errors, cases α, β .

Table 1

=====

Example for cases, where the limits of validity of an empirical absorption function are not observed.

empirical relation : $A = \int A_{\nu} d\nu = 18 (m \cdot p^{0.7})^{0.53}$ for 2224 N₂O - band.

limits of validity : $10 < A < 45$ in combination with another equation, valid for $A \geq 45$, one obtains the correct values : cases (α), (γ)

if one goes to $10 < A < 79$ and does not use in the time another equation, which is valid for $A \geq 45$, one obtains the wrong values of case : (β)

if one goes to $10 < A < 141$ and does not use in the time another equation, which is valid for $A \geq 45$, one obtains the wrong values of case : (δ)

	(α)	(β)	(γ)	(δ)
H ₂ O	H ₂ O, CO ₂	H ₂ O, CO ₂ , N ₂ O-9	H ₂ O, CO ₂ , N ₂ O-3	H ₂ O, CO ₂ , N ₂ O-3
F · 10 ⁺⁶	0,6605	0,3329	0,3117	0,3657
T _a	283,8	276,0	265,5	269,2
				269,0

gases : H₂O, CO₂, N₂O ; N₂O-3 designates that we have taken 3 times the N₂O - mass originally used and given in table 4 (similar meaning of N₂O-9)

outgoing radiation : F [watts · cm⁻¹]

equivalent temperature : T_a [°K]

II.b) Application of the transmission functions in smaller spectral regions (also in overlapping cases).

We calculate the outgoing radiation in the following spectral regions:

- (a) 1210 - 1410 (cm^{-1})
- (b) 2030 - 2290 (cm^{-1})
- (c) 2625 - 3225 (cm^{-1})

where as absorbing atmospheric molecular gases are present:

- (a) H_2O , N_2O , CH_4
- (b) H_2O , CO_2 , N_2O , CO
- (c) H_2O , CH_4 .

For H_2O and CO_2 we use the Plass-tables, from which we calculate mean values $\bar{\tau}$ of transmission for our spectral ranges despite the critic which has been given to the accuracy of these values. As the transmission in these tables is given as function of the three variables P, w, T, we have to interpolate in diagrams like those given in fig. 1.

For N_2O , CH_4 , CO we use the experimental data of Burch and al. (Ref. 31) and the experimental data of Goody and Wormell (Ref. 43). For the time being we have not applied any temperature correction to these experimental data. As Goody and Wormell and List and Oppel (Ref. 40) have shown, the temperature dependence of a single absorption band can be neglected. The temperature variation in the atmosphere is not large, the temperature has a more pronounced effect on the strength of the spectral lines. Nevertheless, we use a temperature reduction for H_2O and CO_2 , as the Plass-tables are given with respect to temperature. We take

$$[5] \quad T_{\text{reduced}} = \frac{\sum \Delta_m \cdot \bar{T}}{\sum \Delta_m}$$

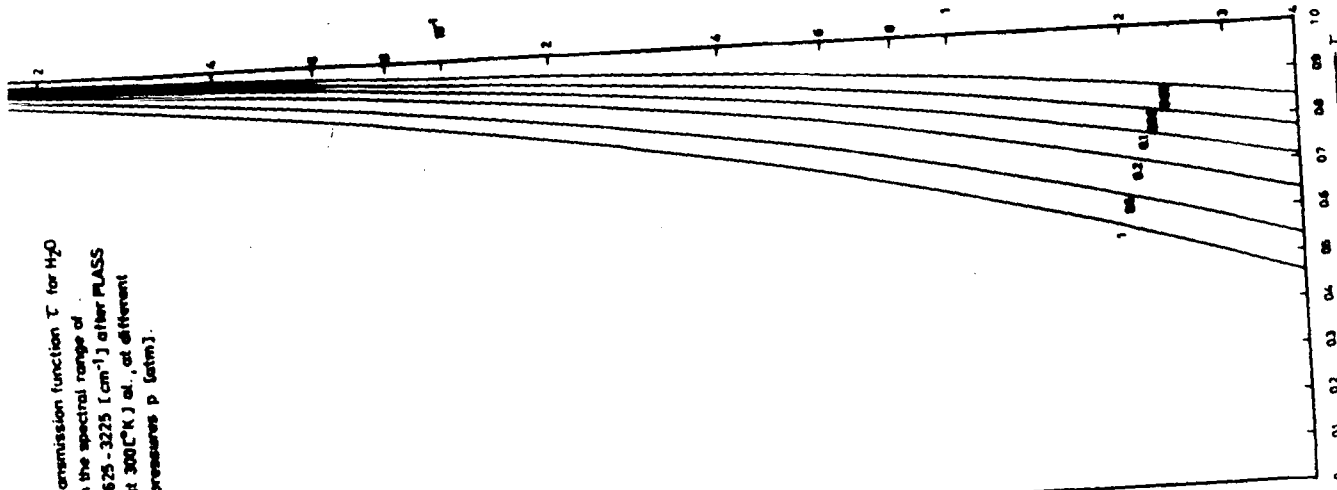
as Bolle (Ref. 41) has used.

Δ_m = difference of absorbing mass between two levels

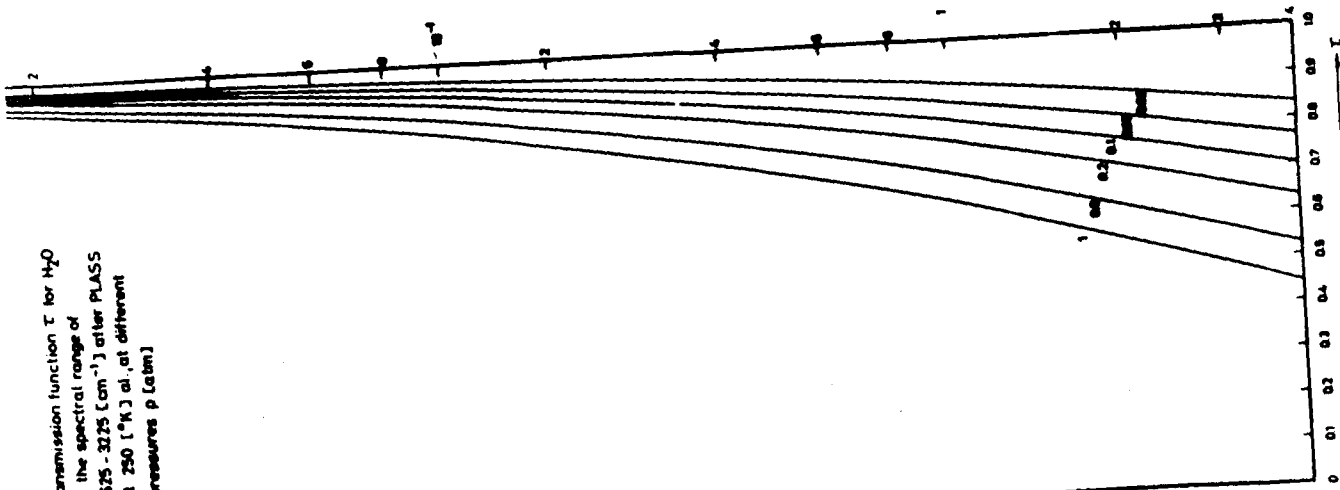
$\bar{T} = (T_i + T_{i+1}) \cdot \frac{1}{2}$, where T_i = temperature in the i-th level.

Fig. 1

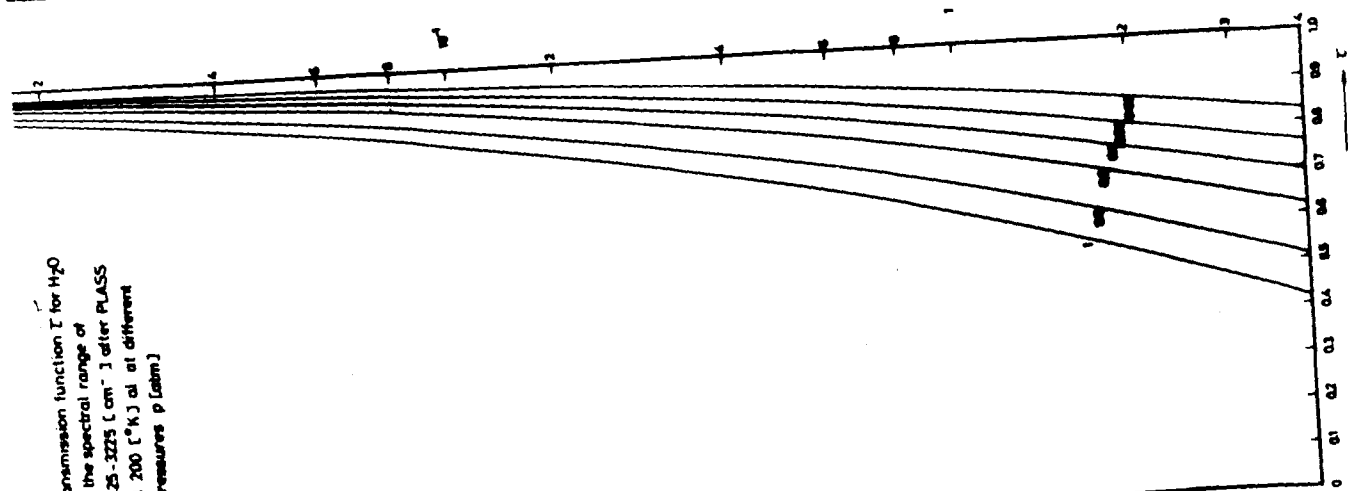
Transmission function T for H_2O
in the spectral range of
2625 - 3225 (cm^{-1}) after PLASS
at 300 $(^{\circ}K)$ at different
pressures p (atm).



Transmission function T for H_2O
in the spectral range of
2625 - 3225 (cm^{-1}) after PLASS
at 250 $(^{\circ}K)$ at different
pressures p (atm).



Transmission function T for H_2O
in the spectral range of
2625 - 3225 (cm^{-1}) after PLASS
at 200 $(^{\circ}K)$ at different
pressures p (atm).



For pressure correction we use according to Curtis (Ref. 34, 35, 36, 45)

$$[6] \quad P_{\text{reduced}} = \frac{\sum \bar{P} \Delta m}{\sum \Delta m}$$

where $\bar{P} = 1/2 (P_i + P_{i+1})$.

When more than one absorber are present, the outgoing radiation F is calculated by means of multiplication of the transmissions of the individual gases:

$$[7] \quad F(\bar{\tau}_1, \bar{\tau}_2, \dots, \bar{\tau}_n) = F(\bar{\tau}^*)$$

where $\bar{\tau}^* = \prod_{j=1}^n \bar{\tau}_j$

$\bar{\tau}_j$ = mean transmission of the j -th gas in the regarded spectral interval. The influence of the different gases on the vertical distribution of $\bar{\tau}^*$ can be seen in fig. 2: it gives the transmission of the atmosphere as it is seen from 31 km altitude to given pressure levels below. Our curves show remarkable absorption of CO_2 and N_2O yet at greater heights. As we have used a relatively small value for the mixing ratio of N_2O , this absorption could be yet greater in reality.

II.c) Planck function as term of the equation of radiative transfer.

In an accurate calculation one has to take the black body radiation $B_\nu = B_\nu(T)$ at every frequency of the absorption band and multiply it with the specific transmission of the related wave number. But the so-called "spectral calculation" necessitates a large effort in computer time. If one takes a mean transmission function over a number of frequencies one also can take a mean value of the black body radiation in the regarded spectral interval. The choice of such a mean value of the black body radiation in one spectral interval is not easy: the distribution of the transmission functions of the gases are superposed by the radiation which is emitted

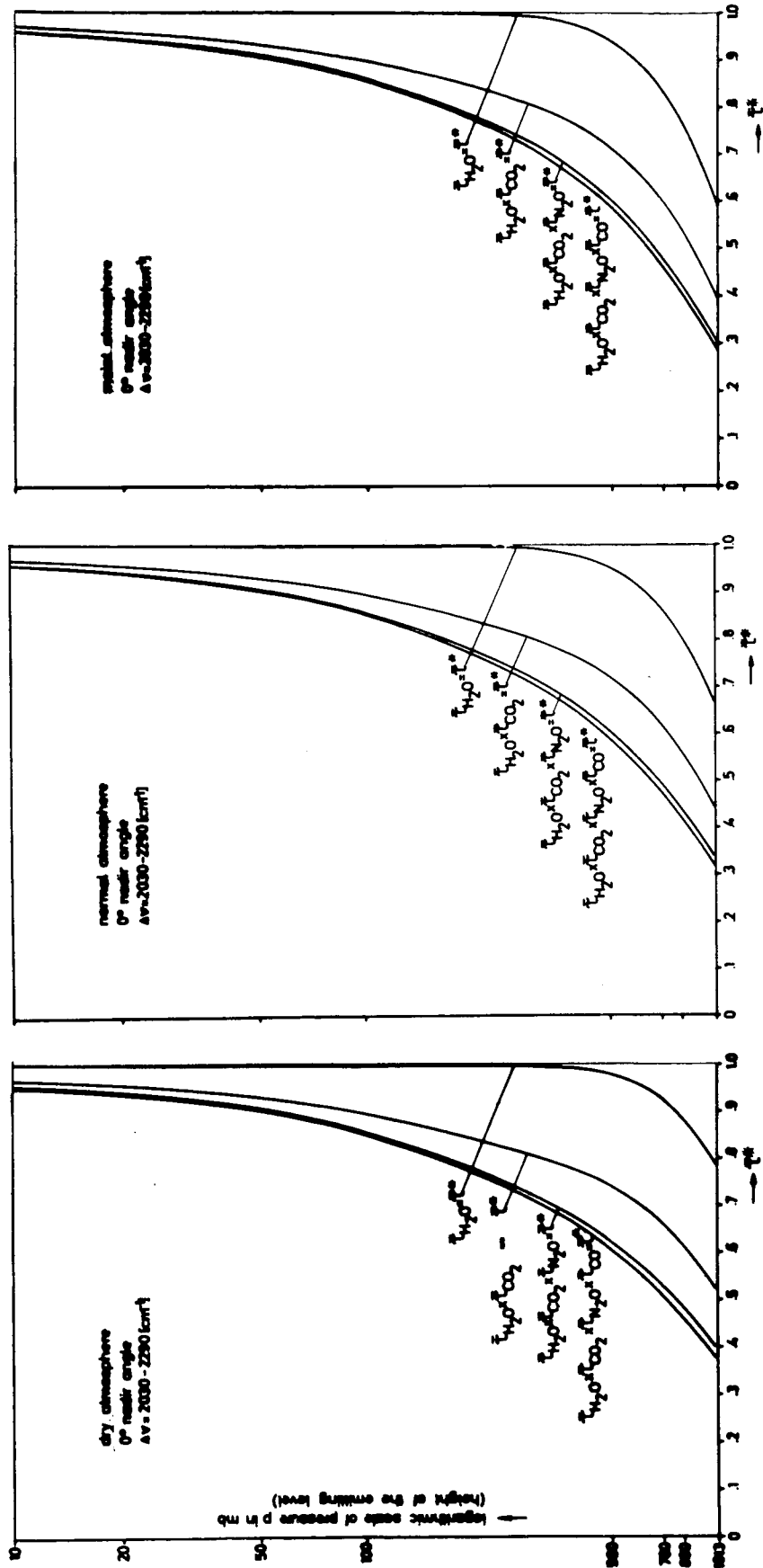


Fig. 2: Transmission τ^* of layers with growing thickness, starting from 10 mb ($\approx 31 \text{ km}$) altitude to the Earth surface. The influence of different gases is investigated.

by the Earth surface. To determine a mean value $\bar{B}_{\Delta\nu}$ one should know the distribution of the outgoing radiation as a function of the frequency: $F_\nu = F_\nu(\nu)$. Then one could take

$$[8] \quad \bar{\epsilon}_{\Delta\nu} \cdot \bar{B}_{\Delta\nu} = \bar{F}_{\Delta\nu} \quad ,$$

where $\bar{F}_{\Delta} = \frac{1}{\Delta\nu} \int_{\Delta\nu} F_\nu d\nu$ and $\bar{\epsilon}_{\Delta\nu} = \frac{1}{\Delta\nu} \int_{\Delta\nu} \epsilon_\nu d\nu = \frac{1}{\Delta\nu} \int_{\Delta\nu} \frac{F_\nu}{B_\nu} d\nu$ is

the mean value of the "emissivity" of the atmosphere, including the radiation which originates from the Earth surface or from clouds. (These considerations follow an idea which Bolle (Ref. 41) has used in his calculations of the emission of the atmosphere at the ground). But our conditions become complicated, as we have to regard that most of the outgoing radiation at 10 mb does not come from the 10 mb level but from other heights. If one knows from which level most of the radiation is coming from (in one spectral range), one should have measurements of $F_\nu(\nu)$ at this level and then operate after equation [8].

These considerations show that it would be very difficult to get any indication about the frequency ν_s at which B_{ν_s} could be regarded as weighted mean value in the whole respective spectral interval. Therefore, we have generally taken for ν_s the arithmetic mean value of ν in the interval $\Delta\nu = \nu_2 - \nu_1$.

$$[9] \quad \overline{B_\nu(T)} = B_{\nu_s}(T)$$

$$\nu_s = \frac{\nu_1 + \nu_2}{2} = \nu_{arith} \quad .$$

Now we may calculate $F_{\Delta\nu}(\nu_s)$ according to equation [1].

Then we have studied the error of this choice: We have calculated F as function of the blackbody radiation B for different values of ν_s (deviating from the arithmetic mean value) fig. 3a. The difference is severe. But if one calculates the attached equivalent blackbody temperatures from F at those frequencies ν_s , the difference is not very severe: fig. 3b.

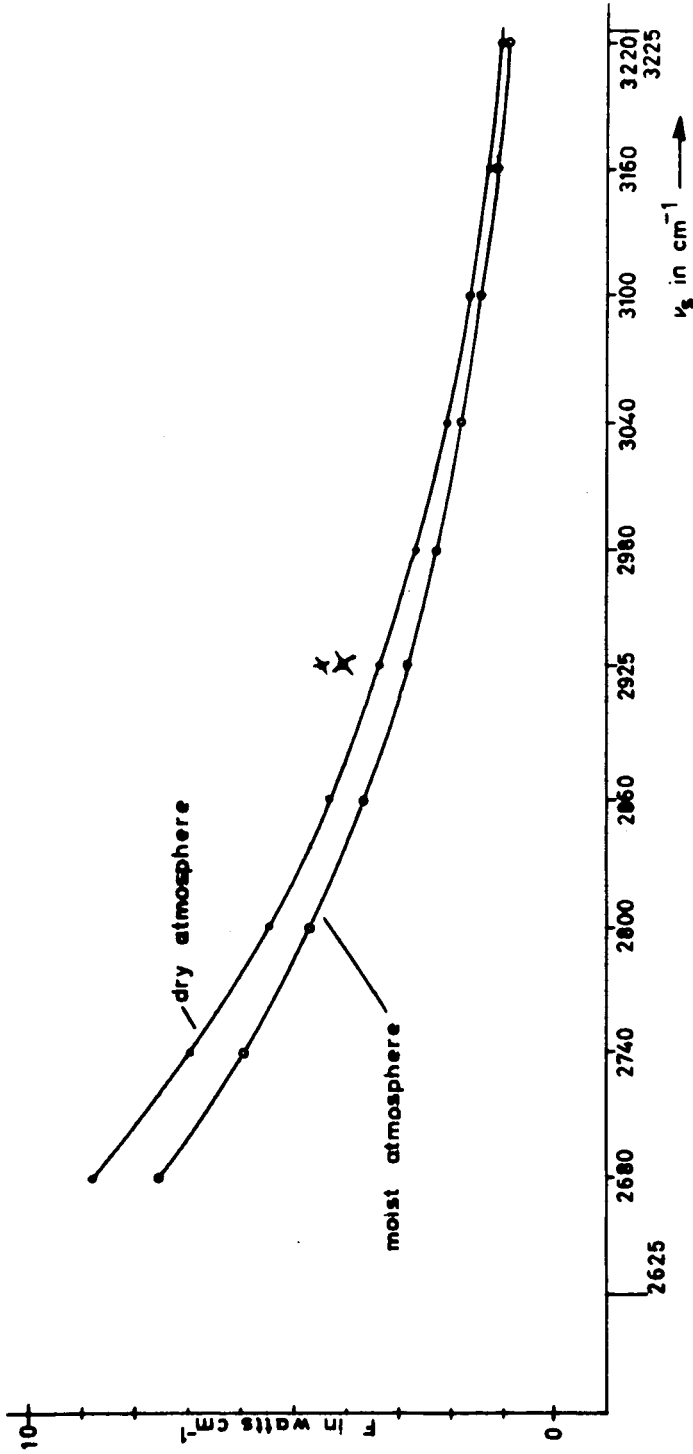


Fig. 3a: $\Delta \nu = 2625 - 3225 (\text{cm}^{-1})$, 0 degrees nadir angle.

Outgoing radiation F at 10 mb. The influence of the choice of ν_s (the frequency parameter in the Planck-function) is shown. Points \times , \times are obtained by subdivision of the spectral range $\Delta \nu$ into smaller parts, and are calculated after equation [11].

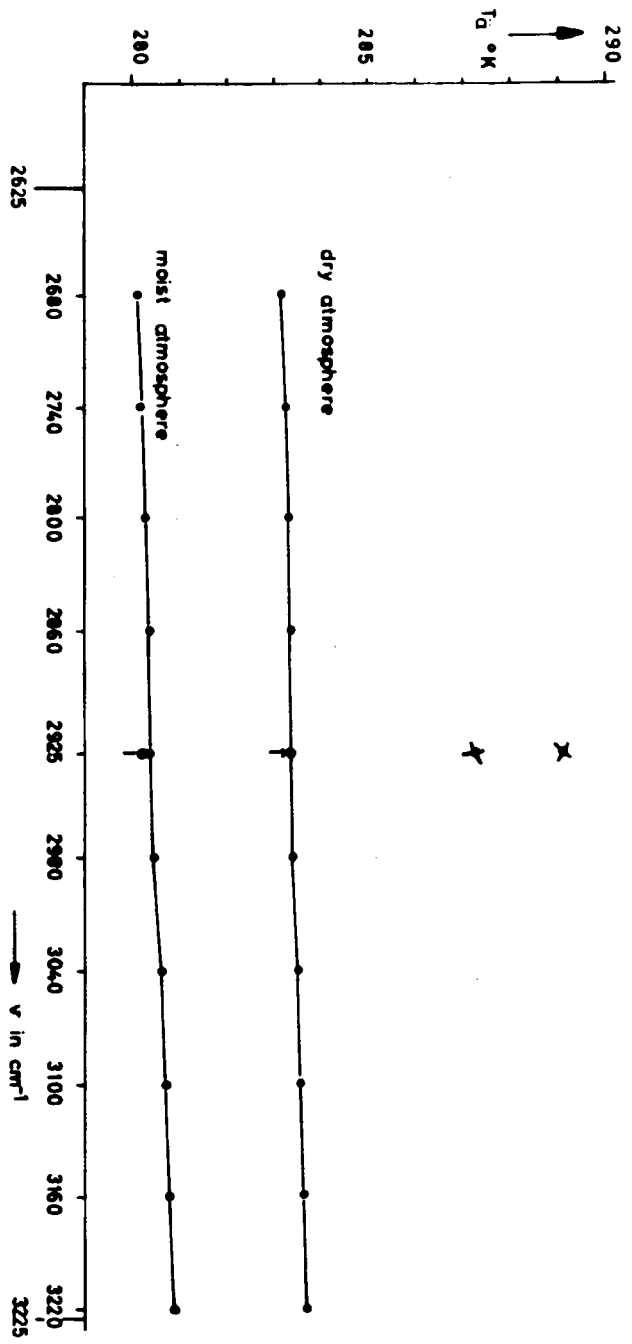


Fig. 3b: $\Delta\nu = 2625 - 3125$ (cm $^{-1}$), 0 degrees nadir angle.

Influence of the choice of ν_s (= frequency parameter in the Planck-function) on the equivalent temperature T_g which is attached to the outgoing radiation in Fig. 3a.

points 'x' are calculated after equation [12] with $\bar{\nu}_s = \nu_{arithm}$,
 points 'y' are calculated after equation [13],
 all other points are calculated after equation [1].

After this, we have studied the error of the choice of v_s on the outgoing radiation F by dividing the original Δv into smaller parts:

$$[10] \quad v = \sum_i \Delta v_i$$

we calculate

$$[11] \quad \bar{F}_{\Delta v} = \frac{1}{\sum \Delta v_i} \cdot \sum_i \Delta v_i \cdot F_{\Delta v_i} ,$$

where v_{s_1}, \dots, v_{s_n} are the mean values of v in the sub-intervals $\Delta v_1, \Delta v_2, \dots$ and where $F_{\Delta v_i}$ are already weighted by the length of the attached spectral interval. The difference between $\bar{F}_{\Delta v}$ and $F_{\Delta v}$ is not extreme severe, but nevertheless noticeable fig. 3a.

But if one calculated the equivalent temperature from $\bar{F}_{\Delta v}$ for the interval v one has to choose now a v_s in Δv :

$$[12] \quad \bar{F}_{\Delta v} \leftrightarrow \bar{v}_s .$$

If one now takes $\bar{v}_s = v_{arithm}$ one would have a very large error: fig 3b. This error (ΔT) would in general exceed the error ($\Delta \bar{T}$) due to the choice of v_s in the calculation without subdivision of Δv , especially when the bands have an asymmetric distribution in the spectral interval, fig. 3b, table 2. Therefore, if one wants to get more exact values for $T_{\bar{a}}$ by subdivision into smaller parts one has first to calculate $T_{\bar{a}}(\Delta v_1), T_{\bar{a}}(\Delta v_2) \dots$ and then to form from them the mean value $\bar{T}_{\bar{a}}$, fig. 3b. $T_{\bar{a}}$ must be weighted with the length of the attached spectral interval.

$$[13] \quad T_{\bar{a}} = \frac{1}{\sum_i \Delta v_i} \cdot \sum_i \Delta v_i \cdot T_{\bar{a},i} ,$$

where i = number of sub-intervals.

Table 2
=====

Equivalent temperatures from different sorts of calculations.

$\Delta \nu = 2625 - 3225 \text{ cm}^{-1}$

		H ₂ O, N ₂ O, CH ₄	H ₂ O, N ₂ O	H ₂ O
(A)	$T_{\text{g}} = f [F_{\Delta \nu} (\nu_{\text{arith}})]$ where $F_{\Delta \nu}$	283.4	284.8	284.8
	after equation [1]	281.5	283.0	282.9
(B)	T_{g} after equation [13]	280.4	281.8	281.8
(C)	$T_{\text{g}} = f [\bar{F}_{\Delta \nu} (\nu_{\text{arith}})]$ where $\bar{F}_{\Delta \nu}$	283.3	284.8	284.8
	after equation [11]	281.2	282.7	282.7
$\Delta T = T_{\text{g}} (A) - T_{\text{g}} (B)$	d	279.9	281.3	281.3
	n			
$\Delta T = T_{\text{g}} (C) - T_{\text{g}} (B)$	d	289.1	290.2	290.2
	n	287.9	289.0	289.0
$\Delta T = T_{\text{g}} (C) - T_{\text{g}} (B)$	f	287.2	288.2	288.2
	d			
$\Delta T = T_{\text{g}} (A) - T_{\text{g}} (B)$	d	+0.1	+0.0	+0.0
	n	+0.3	+0.3	+0.2
$\Delta T = T_{\text{g}} (C) - T_{\text{g}} (B)$	f	+0.5	+0.5	+0.5
	d			
$\Delta T = T_{\text{g}} (C) - T_{\text{g}} (B)$	d	+5.8	+5.4	+5.4
	n	+6.7	+6.3	+6.3
$\Delta T = T_{\text{g}} (C) - T_{\text{g}} (B)$	f	+7.3	+6.9	+6.9
	d			

where d = dry atmosphere, n = normal atmosphere, m = moist atmosphere according to table 3.

The absorption coefficients of different gases are different functions of pressure, mass, and temperature. Therefore, one had to choose exactly at every level j another ν_s for the calculation of ${}_j B_{\nu_s}$. If one wishes to investigate the influence of single gases one has to take for each gas which is added another ν_s : calculating at a mean value of ν_s will generally have the consequence that the absorption of the one or the other gas is preferred. This may already be seen from fig. 5, where we compare calculations for the interval 1210-1410 (cm^{-1}) obtained from equation [9] with those from [12]. If one calculates only with the absorption of water vapor and after [9] one gets an equivalent temperature $T_{\bar{a}}$ which is smaller compared with the value obtained if first the interval is subdivided into smaller parts but choosing the wrong ν_s after [12]. If one now regards H_2O and N_2O one gets the same value for $T_{\bar{a}}$ with and without spectral subdivision. If one finally regards H_2O , N_2O and CH_4 , $T_{\bar{a}}$ grows larger against the value after [12].

In the spectral range 2625 - 3225 (cm^{-1}) at the short wave limit of this interval, there is the relatively strong 3020 (cm^{-1}) CH_4 -band, overlapped by the wing of the 2.7 micron H_2O -band, while there is no strong absorption at the long wave limit of this interval. By calculating after [12] not only the relative amount of the influence of the CH_4 on $T_{\bar{a}}$ will be calculated erroneously, but of course also the absolute value of $T_{\bar{a}}$, fig. 4. The strong asymmetry of the absorption bands may lead here to an error of 6 degrees!

In this spectral region 2030 - 2224 (cm^{-1}) the absorption seems to be situated favourably to ν_s concerning the absorption of the different gases: The values of F respectively $T_{\bar{a}}$ obtained with [9] and [12] have a relatively small difference, fig. 6. Similar consideration can be made in the other spectral intervals, fig. 7, fig. 8. One may conclude that generally the results will be more accurate if it is calculated with

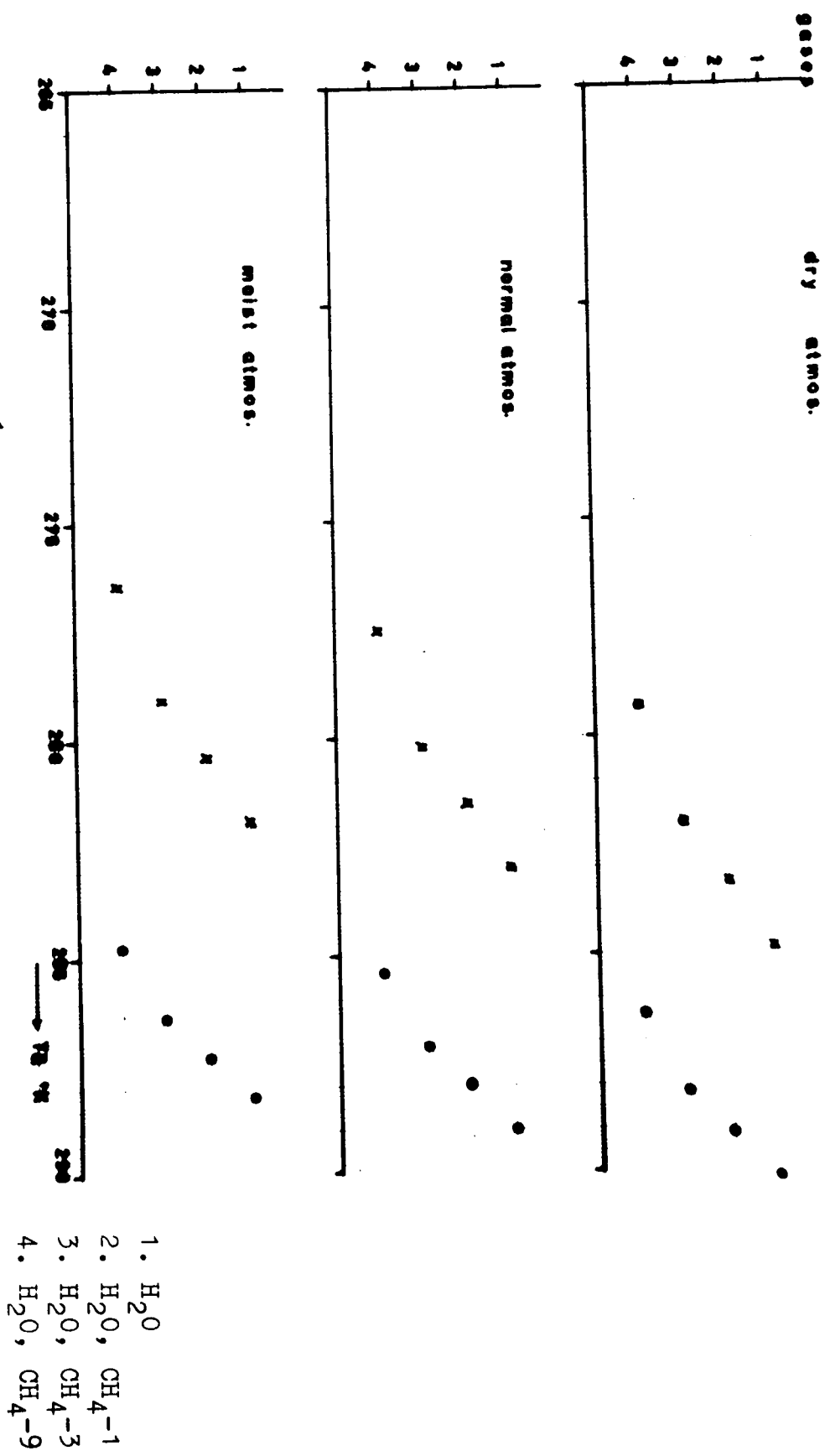


Fig. 4: $\Delta\nu = 2625 - 3325$ (cm^{-1}), 0 degrees nadir angle.
 Equivalent temperature T_g for the outgoing radiation at 10 mb. Absorption quantities are varied. The number on the ordinate indicate the regarded gas. The number behind the gas symbol indicates, how many times we have taken the original mass of this gas.

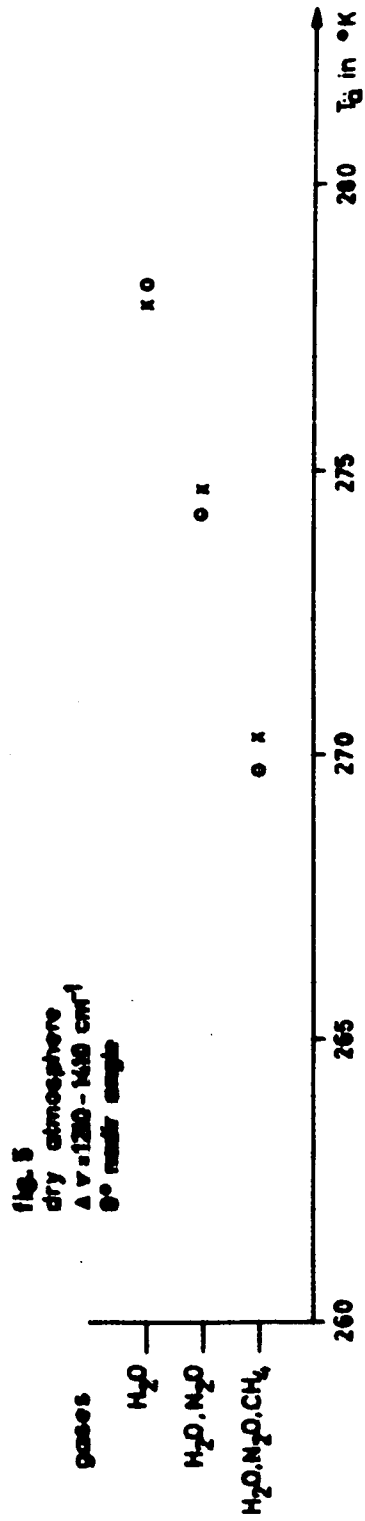


Fig. 5: Equivalent temperature T_g for the outgoing radiation F at 10 mb.

points X calculated after equation [1] and relation [9]

points O calculated after relation [11] and [12] at $\bar{v}_s = v_{\text{arithm}}$.

Fig. 6

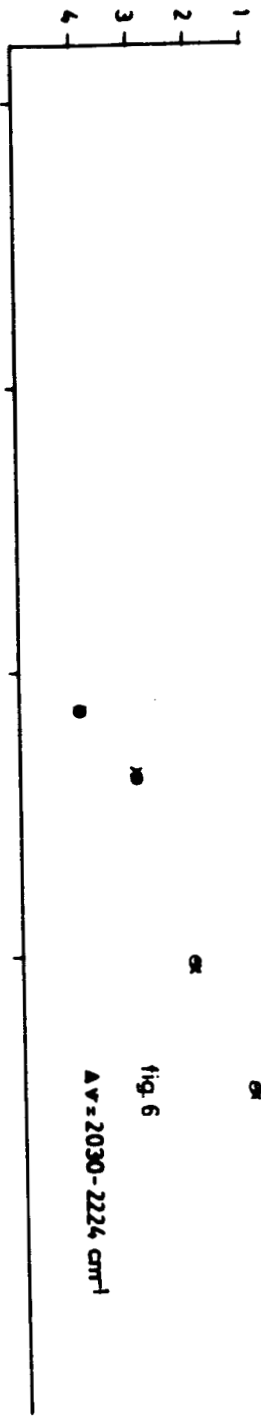
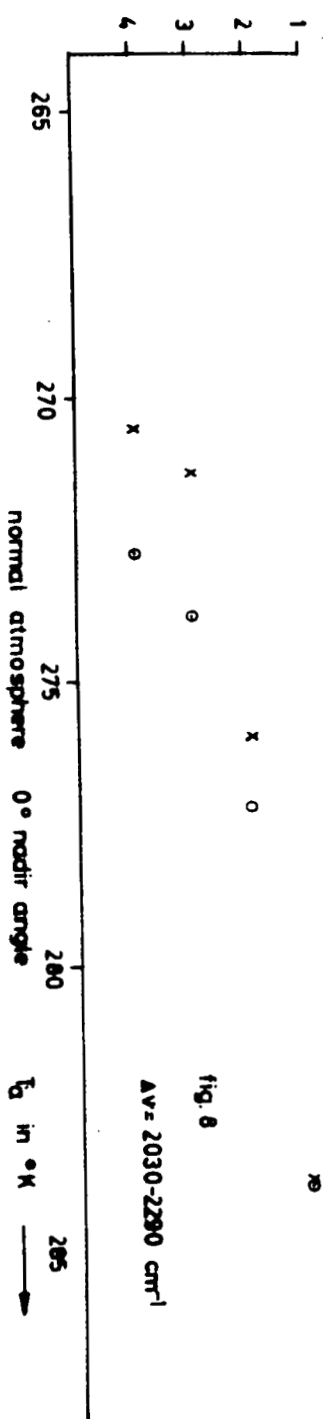


Fig. 7



Fig. 8



Equivalent temperature T_i for the outgoing radiation F at 10 mb, when different gases are regarded. The number behind the gas symbol indicates, how many times we have taken the original mass of this gas.

- 1: H₂O
- 2: H₂O, CH₄ - 1
- 3: H₂O, CH₄ - 3
- 4: H₂O, CH₄ - 9

points x are calculated by means of equation [1] when $v_s = v_{arith}$.
 points o are calculated by means of equation [11].

smaller spectral intervals and take [13] for the determination of the equivalent temperature.

II.d) Vertical distribution of atmospheric gases and their influence on the upward directed radiation in the atmosphere.

Our calculations have been made on the basis of the U.S. Standard Atmosphere 1962 (Ref. 47). To vary the water vapor content, we have varied the mixing ratio c according to table 3.

In this table the numbers c_{normal} give the values from the U.S. Standard atmosphere 1962

To get probable values of the vertical distribution of CO_2 and the minor atmospheric constituents, we oriented us by different authors.

The mixing ratios for these gases have been supposed to be constant with height.

The mass Δm of an absorbing layer has been calculated by the formula

$$\Delta m = \frac{\bar{c}_i \cdot M_{\text{gas}} \cdot 10^{-3} \cdot \Delta p}{g \cdot M_L \cdot \rho_{N,\text{gas}}} = \frac{\bar{c}_i \cdot 22.4 \cdot \Delta p}{g \cdot 28.966} \quad [\text{atm-cm}]$$

where

\bar{c}_i = mean mixing ratio of the regarded gas in the i -th layer

$g = 981 \text{ (cm} \cdot \text{sec}^{-2}\text{)}$

$M_L = 28.966$ = molecular weight of dry air

M_{gas} = molecular weight of the regarded gas

$\rho_{N,\text{gas}}$ = specific weight of the regarded gas at NTP

22.4 = volume of one Mol per litre.

$\Delta p = (p_i - p_{i+1})$ in mb

With these values we have calculated the outgoing radiation. As can be seen from table 4, there is no general agreement

Table 3
=====

Vertical distribution of water vapor; mixing ratio c [$\text{cm}^3 \cdot \text{m}^{-3}$] ; p = pressure [mb]

p	c (dry)	c (normal)	c (moist)
1013	2700	6150	9490
795	1260	3200	5090
585	420	1360	2150
470	192	688	1117
350	35,9	234	376
250	8,6	37,0	66,6
190	7,5	16,6	26,7
130	8,2	9,7	12,3
110	8,6	9,2	9,7
70	12,8	15,1	12,8
50	18,6	21,4	18,6
30	43,2	43,1	43,2
10	165	150	165

total water vapor
mass [$\text{g} \cdot \text{cm}^{-2}$]

0,6578

1,6716

2,6741

Table 4

=====

Mixing ratio c [$\text{cm}^3 \cdot \text{m}^{-3}$] and total content (atm - cm) of atmospheric cases.

Author	Year	CO ₂	N ₂ O	CH ₄	CO
Goody	1958	300	0,35	2	0,2
Seeley, Houghton	1961	-	0,12	1,05	0,12
Howard, Garing	1962	320	0,27	2,4	[1,1]
Bowman, Shaw	1963	-	0,28	1,7	[1,3]
Goldberg, Müller	1951 (1953)	-	0,5	1,5	-
Glückauf	1963	-	-	1,2	-
Shaw	1959	-	0,28(±0,04)	2,4	-
Migeotte, Neven	1952	-	-	-	0,19-0,29
Linke	1953	300	0,5	2,2	-
Benesch, Migeotte	1953	-	-	-	0,031-0,14
Locke, Herzberg	1953	-	-	-	0,11-0,22
					0,19
					0,15
					0,16
Shaw	1959	-	-	-	0,13
Miller	1956	-	0,5	-	-

Table 4 (continued)
 =====

Author	Year	CO ₂	N ₂ O	CH ₄	CO
Goody, Walshaw	1953	-	0,27(±0,08)	-	-
Slobod, Krog	1950	-	0,25-0,65	-	-
Birkeland	1957	-	0,39-0,57	-	-
Hagemann	1959	311± 2	-	-	-
Keeling	1960	313	-	-	-
Foltzik, Hinzpeter	1958	332	0,4-0,6	2,2	-
Georgii	1963	-	0,2-0,6	-	-
Howard		300	0,5	-	-
		-----	-----	-----	-----
mean value		312,6	0,40	1,8	0,18
we have used	1964/65	313	0,30	1,6	0,2
<u>total content (atm - cm) :</u>		246	0,236	1,11	0,158
3 times			0,708	3,33	0,474
9 times			2,124	9,99	1,422

concerning the masses of the minor constituents in the atmosphere. Therefore, we have calculated the outgoing radiation for different absorber masses to show their influence on the outgoing radiation and on the equivalent temperatures, see fig. 9 - 12. In these figures the number behind the gas-symbol indicates how many times we have taken the absorber mass, originally used according to table 4, and the designation dry, normal, moist atmosphere relate to the values of c in table 3.

One can see that greater errors in absorption mass would lead to significant errors in the equivalent temperatures. In fig. 4 - 6 there has been plotted the outgoing radiation in relation to the case, when water vapor respectively water vapor and carbon dioxide are the only gases.

III. RESULTS AND CONCLUSIONS.

We have shown that a remarkable misinterpretation of measurements of the outgoing radiation in smaller spectral ranges can be caused by the following errors in the calculation of the outgoing radiation:

- 1) neglect of minor atmospheric constituents
- 2) uncertain values of mixing ratio
- 3) calculation with mean values of transmission functions and of the blackbody radiation function
- 4) inaccuracy of the transmission function (see section IIa).

The amount of the influence of the last error we have not yet investigated as extensive as the others in our spectral ranges; comparisons in several spectral ranges could be done with the aid of references 42, 52. The amounts of the errors mentioned under 1), 3) have been found to be about

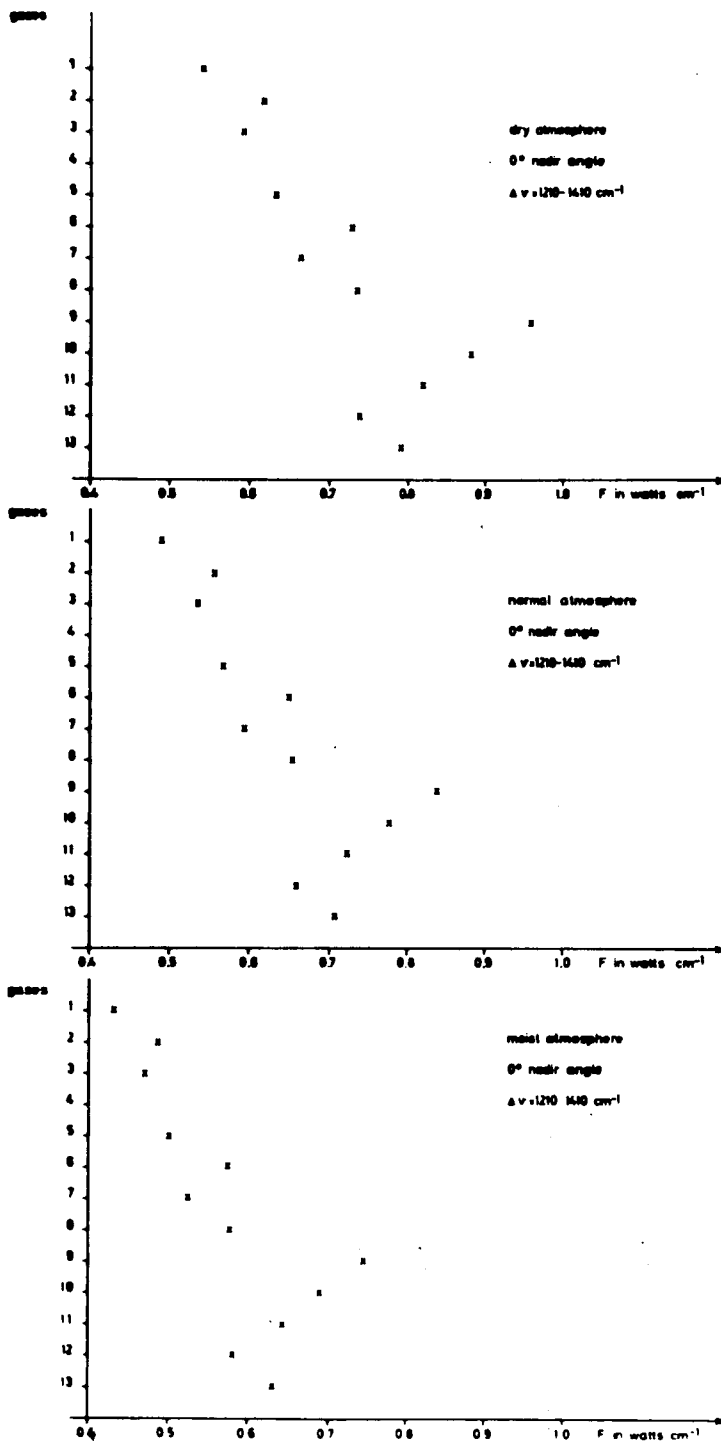
spectral range	1)		3)	
	$\Delta T [^{\circ}K]$	$\Delta Q [\%]$	$\Delta T [^{\circ}K]$	$\Delta Q [\%]$
$\Delta \nu = 1210 - 1410$:	8°	18	0.5	2.5
$\Delta \nu = 2290 - 2030$:	5	20	2	1
$\Delta \nu = 2625 - 3225$:	2	8	6	0.04

where ΔT in $^{\circ}K$ is the error of the amount of the equivalent temperature and ΔQ is the error when the outgoing radiation F is regarded in relation to that value of F , when water vapor and CO_2 are the only absorbing gases. The influence of the errors mentioned under 3) should be taken from the figures.

In the spectral range 2625 - 3225 (cm^{-1}) we have raised the height of the emitting level. We have found that a neglect of the CH_4 -absorption and emission leads to a value of the equivalent temperature which is too high by ΔT in comparison to that value which one obtains without this neglect.

p(mb)	$\Delta T [^{\circ}K]$
1013	1.6
950	1.4
710	1.1
410	0.5

where p = pressure at the height of the emitting level.



1. H₂O, N₂O-9, CH₄-9
2. H₂O, N₂O-9, CH₄-3
3. H₂O, N₂O-3, CH₄-9
4. H₂O, N₂O-3, CH₄-3
5. H₂O, N₂O-1, CH₄-9
6. H₂O, N₂O-1, CH₄-3
7. H₂O, N₂O-9, CH₄-1
8. H₂O, N₂O-3, CH₄-3
9. H₂O
10. H₂O, N₂O-1
11. H₂O, N₂O-3
12. H₂O, N₂O-9
13. H₂O, N₂O-1, CH₄-1

Fig. 9: Outgoing radiation F at 10 mb. Absorber quantities are varied. The numbers on the ordinate are regarded as gas numbers. The number behind the gas symbol indicates, how many times we have taken the original mass of this gas.

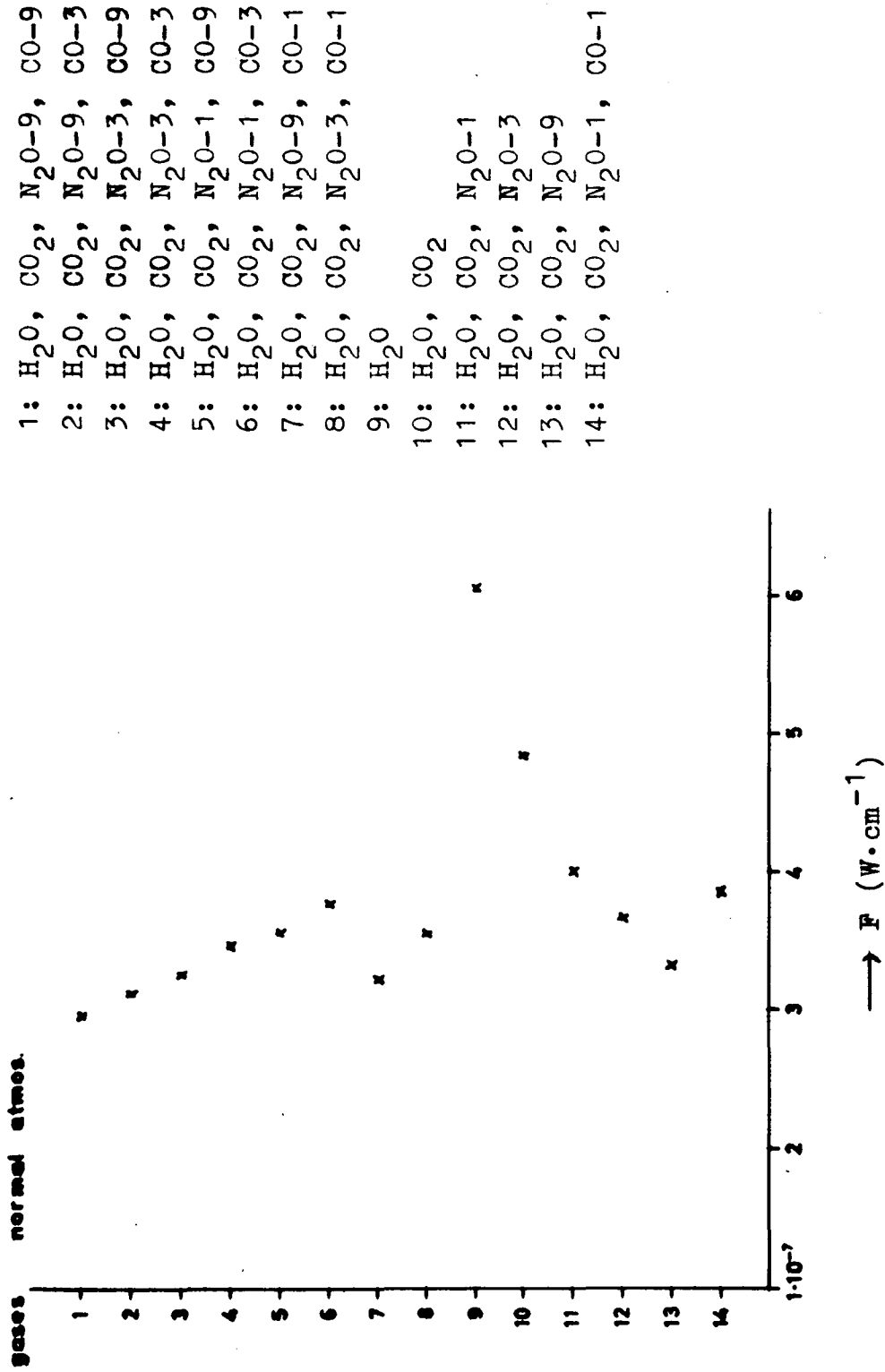


Fig. 11: $\Delta \nu = 2030 - 2290 \text{ (cm}^{-1}\text{)}$, 0 degrees nadir angle. Normal atmosphere: c_{normal}
 Outgoing radiation F at 10 mb. Absorber quantities are varied; the numbers on the ordinate indicate the regarded gases. The number behind the gas symbol indicates, how many times we have taken the original mass of this gas.

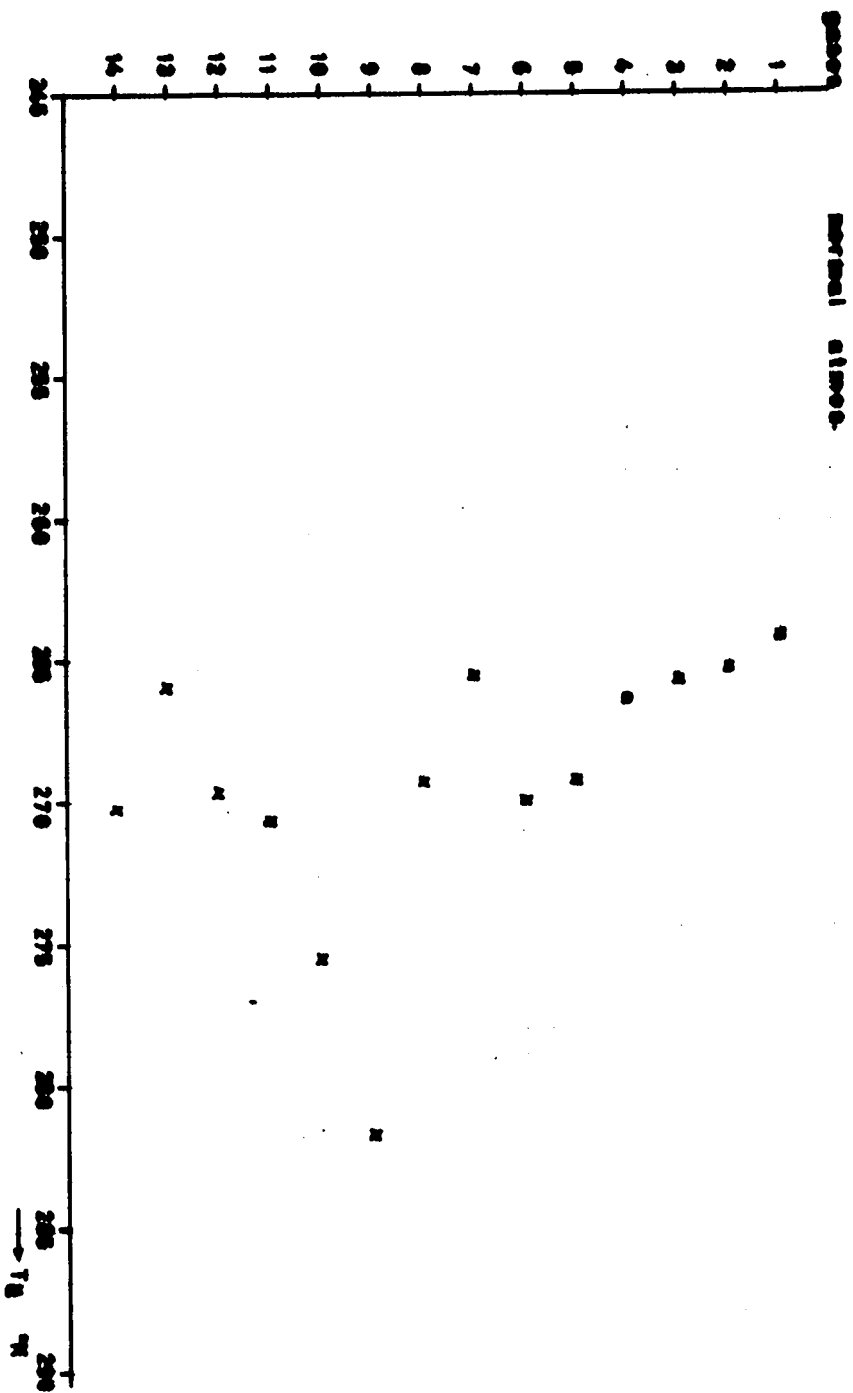


Fig.:12: $\Delta\nu = 2030 - 2290$ (cm^{-1}), 0 degrees nadir angle; normal water vapor distribution.
Equivalent temperature T_g for the outgoing radiation at 10 mb.
Absorber quantities are varied.

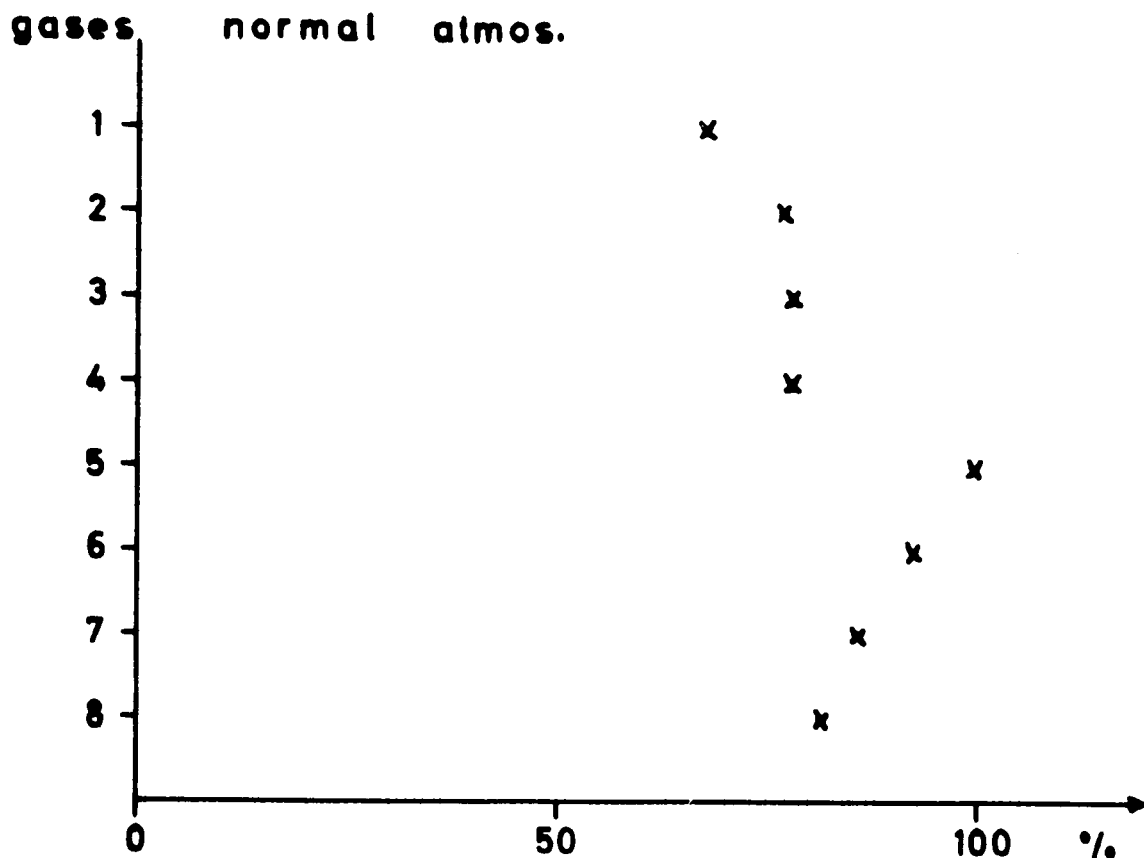


Fig. 13: $\Delta\nu = 1210 - 1410$ (cm^{-1}), 0 degrees nadir angle. Outgoing radiation at 10 mb in relation to the case, when water vapor is the only absorber. Absorber quantities of N_2O and CH_4 are varied. The numbers on the ordinate indicate the regarded gas. The number behind the gas symbol indicates, how many times we have taken the original mass of this gas.

- | | |
|---|---|
| 1: H_2O , N_2O -1, CH_4 -9 | 5: H_2O |
| 2: H_2O , N_2O -1, CH_4 -3 | 6: H_2O , N_2O -1 |
| 3: H_2O , N_2O -9, CH_4 -1 | 7: H_2O , N_2O -3 |
| 4: H_2O , N_2O -3, CH_4 -1 | 8: H_2O , N_2O -1, CH_4 -1 |

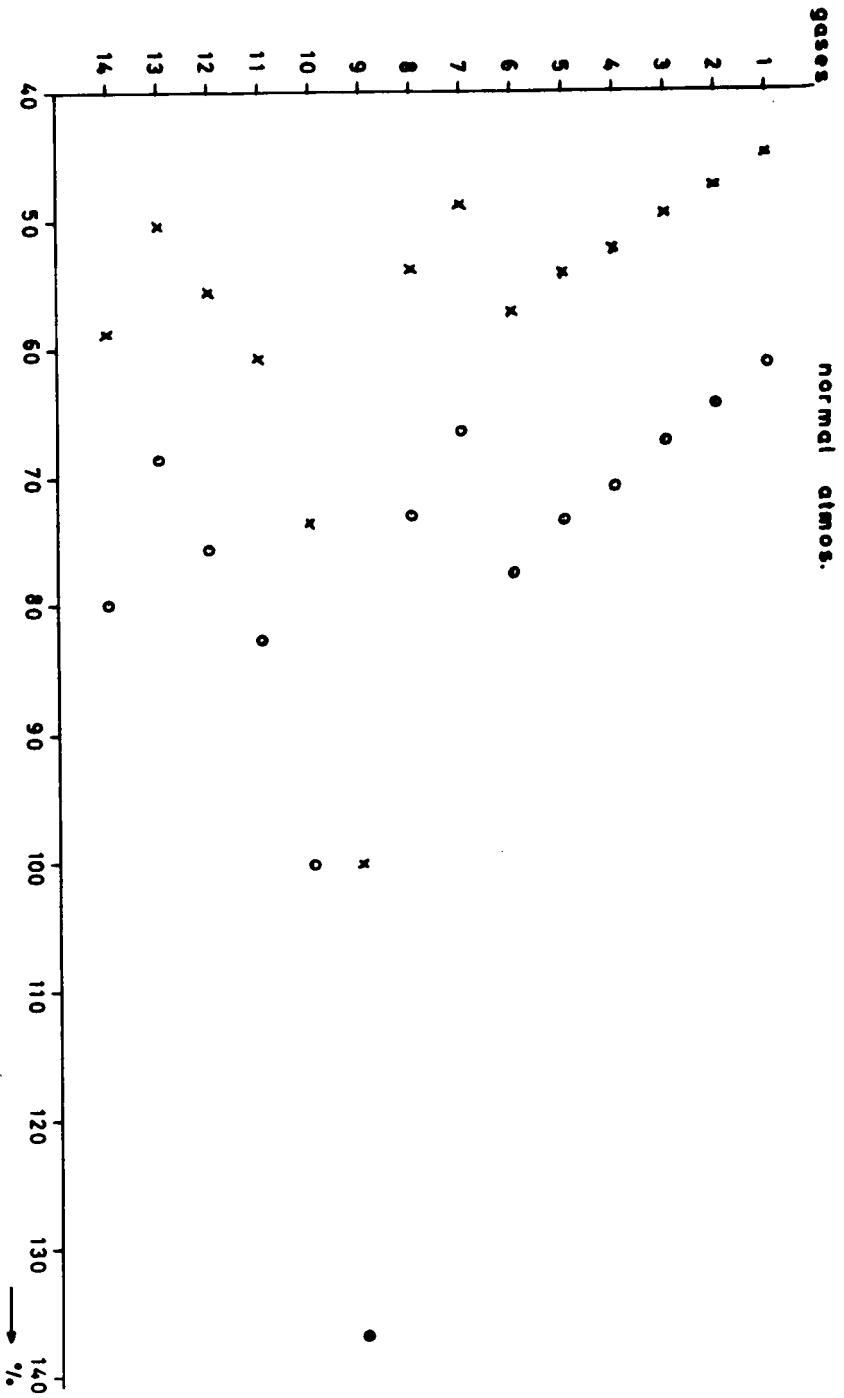


Fig. 14: $\Delta\nu = 2030 - 2290$ (cm^{-1}), 0° nadir angle.

Outgoing radiation when different atmospheric gases are regarded in relation to the case when only water vapor (points X) respectively water vapor and CO₂ (points O) are present. As to ordinate-numbers please see Fig. 11.

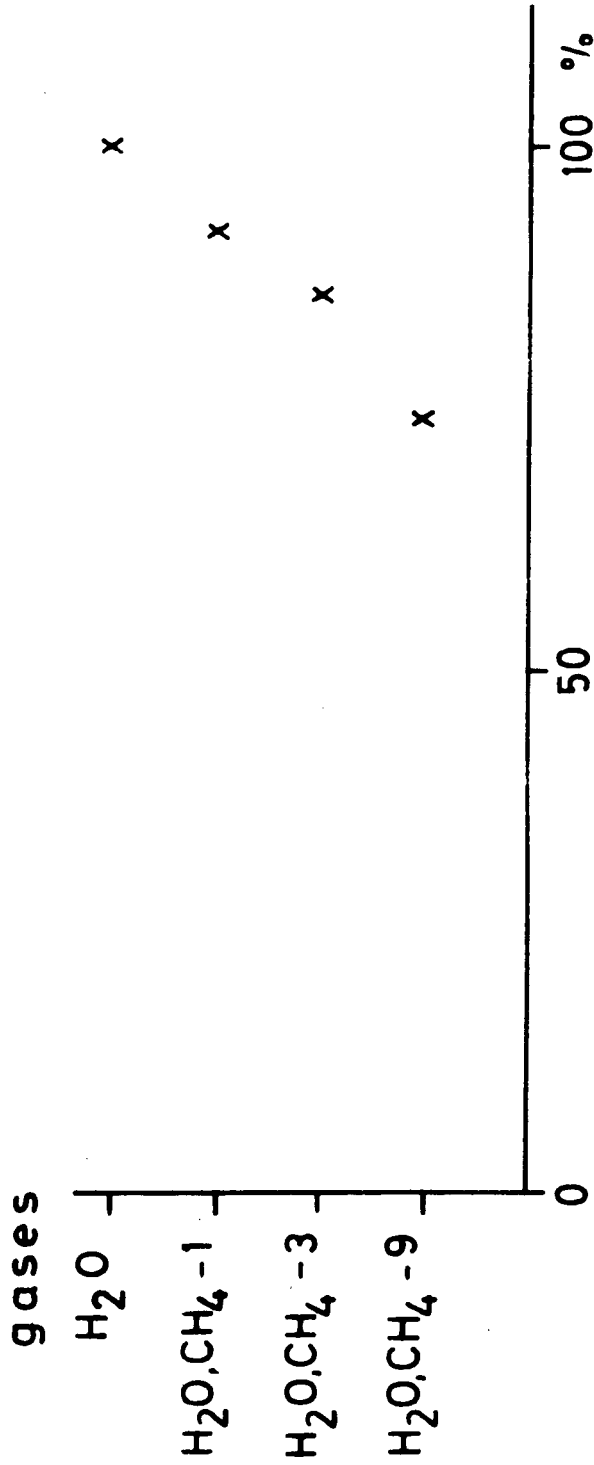


Fig. 15: $\Delta\nu = 2625 - 3225 \text{ (cm}^{-1}\text{)}$; 0° nadir angle.

Outgoing radiation at 10 mb in relation to the case when water vapor is the only absorber. Absorber quantities are varied. The number behind the gas symbol indicates how many times we have taken the original mass of this gas.

IV REFERENCES

1. Bandeen, W.R., Hanel, R.A., Licht, J., Stamfl, R.A., Stroud, W.Q. J. Geoph. Res. 66 (1961), 3169.
2. Bandeen, W.R., Conrath, B.J., Hanel, R.A. : J. Atm. Sci. 20 (1963) s. 609.
3. Wexler, R., Sherr, P. : Synoptic Analysis of TIROS III Radiation Measurements.
AD 431181.
4. Rasool, S.I. : Cloud Heights and Nighttime Cloud Cover from TIROS III Radiation Data.
J. Atm. Sci. 21 (1964), 152.
5. Bandeen, W.R., Halev, M., Strange, I. : A Radiation Climatology in the Visible and Infrared from TIROS Meteorological Satellites.
Intern. Rad. Symp. Leningrad 1964.
6. Möller, F., Raschke, E. : Evaluation of TIROS III Radiation Data. Final Report, March 1964.
7. Wark, D.Q., Alishouse, J., Yamamoto, G. : Variation of the Infrared Spectral Radiance Near the Limb of the Earth.
Appl. Opt. (1964), 221.
8. Hanel, R.A. : Determination of Cloud Altitude from a Satellite.
J. Geoph. Res. 66 (1962), 1300.
9. Yamamoto, G., Wark, D.G. : Discussion of the Letter by R.A. Hanel : Determination of Cloud Altitude from a Satellite.
10. Wark, D.Q. : On Indirect Temperature Soundings of the Stratosphere from Satellites.
J. Geoph. Res. 66 (1961), 77.
11. Wexler, R., Kaplan, L.D. : Simulated Satellite Observations of Atmospheric Infrared Radiation.
A - 59 - 6 - 50 - 144/1/62.
12. Wark, D.Q. : Calculated Infrared Radiation and its Application to Meteorological Satellite Problems.
A - 59 - 6-50-143/1/62.
13. Winston, Y.S., Rao, P.K. : Preliminary Study of Planetary Scale Outgoing Long-Wave Radiation as Derived from TIROS III Measurements.
Month. Weath. Rev. 90 / (1962), 307.

14. Prabhakara, C., Rasool, S.I. : Evaluation of Tiros Infrared Data.
NASA - RP - 80.
15. Marlatt, W.E. : Technical Paper No. 51.
Departm. of Atm. Sci., Colorado State University.
16. Nordberg, W., Bandeen, W.R., Warnecke, G., Kunde, V. : Stratospheric Temperature Patterns Based on Radiometric Measurements from the Tiros VII Satellite.
NASA : X - 651 - 64 - 115.
17. Möller, F. : Einige vorläufige Auswertungen der Strahlungsmessungen von TIROS II.
Archiv für Meteorologie, Geophysik und Bioklimatologie, 12 (1962), 78.
18. Möller, F. : Atmospheric Water Vapor Measurements at 6-7 Microns from a Satellite.
Planet. Space Sci. 5, Pergamon Press, (1961), 202.
19. Kaplan, L.D. : Inference of Atmospheric Structure from Remote Radiation Measurements.
YOSA, 49, (1959), 1004.
20. Wark, D.Q., Yamamoto, G., Lienesch, J.H. : Methods of Estimating Infrared Flux and Surface Temperature from Meteorological Satellites.
J. Atm. Sci. (1962), 369.
21. King, Y.I.F. : Inversion by Slabs of Varying Thickness.
J. Atm. Sci. 21 (1964), 324.
22. Yamamoto, G. : Numerical Method for Estimating the Stratospheric Temperature Distribution from Satellite Measurements in the CO₂ - band.
J. Met. 18 (1961), 581.
23. Drayson, S.R. : Errors in Atmospheric Temperature Structure Solutions from Remote Radiometric Measurements.
Technical Report. University of Michigan. 05863 - 4 - T.
24. Büttner : Regenortung vom Wettersatelliten mit Hilfe von Zentimeterwellen.
Die Naturwissenschaften 50 (1963), 591.
25. Kondrat, Yev, K. Ya. : Some Problems Associated with the Interpretation of the Results of Measuring the Outgoing Radiation by Means of Meteorological Satellites.
NASA - TT - F - 8563.
26. Katz, Y.H. : The Application of passive Microwave Technology to Satellite Meteorology.
(A. Symposium).

27. Drayson, S.R. : A Survey of Progress and Problems in the Kaplan - Experiment.
STAR - N 63 - 21110.
29. Smith, R.A. : Atmospheric Radiative Temperature.
Thesis. University of California at Los Angeles, May 1962.
30. NASA : Nimbus Weather Satellite Scheduled for Launch.
N64 - 27504.
31. Burch, D.E., Gryvnak, D., Singleton, E.B., France, W.L., Williams, D. : Infrared Absorption by Carbon Dioxide, Water Vapor, and Minor Atmospheric Constituents.
AFCRC - 62 - 698.
32. Howard, J.N., Burch, D.L., Williams, D. : Near Infrared Transmission through Synthetic Atmospheres.
Geophys. Res. Pap. No. 40.
AFCRC - TR - 55 - 213.
33. Burch, D. E., Williams, D. : Test of Theoretical Absorption Band Model Approximations.
Appl. Opt. (1964), 55.
34. Godson, W.L. Q.J.R.M.S. 80, (1954), 645.
35. Goody, R.M. : Q.J.R.M.S. 78,(1952), 638.
36. Curtis : Q.J.R.M.S. 80 (1954), S. 645.
37. Kaplan, L.D. : A Method for Calculation of Infrared Flux for Use in Numerical Models of Atmospheric Motion. - The Atmosphere and the Sea in Motion.
The Rossby Memorial, Volume, Oxford 1959, Page 170.
38. Stull, Wyatt, Plass : Infrared Transmission Studies.
SSD - TDR - 62 - 127, Volume II, III, V.
39. Roney, P. : Atmospheric Absorption in the 2 to 5 Micron Region of the Solar Spectrum at 40,000 Feet.
Carde Technical Report, 475.
40. List, L.L., Oppel, G.E. : Atmospheric Transmission from 4 to 5 microns.
AD 446805.
41. Bolle, H.J. : Ausarbeitung eines Verfahrens zur Vorhersage thermischer Strahlung.
Meteorologisches Institut der Universität München.
Bericht III, zum Forschungsauftrag T - 369 - I - 203.
42. Taylor, H.W., Yates, J.H. : Infrared Transmission of the Atmosphere.
AD 240 188. U.S. Naval Research Laboratory, Washington 25, D.C.

43. Goody, R.M., Wormell, T.W. : The Quantitative Determination of Atmospheric gases by Infrared Spectroscopic Methods. Proc. Roy. Soc., A, Vol. 209, 1951, Page 178.
44. Burch, D.E. : Applied Optics 1964, Page 55.
45. Goody, R.M. : Atmospheric Radiation I, Oxford, Clarendon. Press, 1964.
46. Elsasser, W.M., Culbertson, M. : Met. Monogr. Vol. 4, August 1960, No, 23.
47. Howard, J.N., Garing, J.S. : The Transmission of the Atmosphere in the Infrared - a Review. Infrared Physics II, 155, (1962).
48. University of Denver : Infrared Atmospheric Transmittance and Flux Measurements. AD 448953.
49. Shaw, J.H. : A Determination of the Abundance of Nitrous Oxide, Carbon Monoxide, and Methane in Ground Level Air at Several Locations Near Columbus, Ohio. AFCRC - TN - 59 - 428.
50. Junge, Ch.E. : Air Chemistry and Radioactivity. Intern. Geoph.Series, Vol. 4. Academic Press, New York, London, 1963.
51. Bandeen, W.R., Kunde, V., Nordberg, W., Thompson, H.P. : Tiros III meteorological satellite radiation observations of a tropical hurricane. Tellus XVI, (1964), 481.
52. Berlinguette, G.E., Tate, P.A. : Some Short-Range Narrow-Beam Atmospheric Transmission Measurements in the Near Infrared. 1963; Defense Research Board of Canada Report No. 420.
53. Kunde, V. : Theoretical Relationship Between the HRIR Equivalent Blackbody Temperatures and Surface Temperatures in Symposium on Geophysical and Meteorological Observations with the Nimbus I satellite. - To be published as a NASA Special Publication. 1965.
28. Drayson. S.R., Atmospheric Slant Path Transmission in the 15μ CO₂-Band. Technical Report 05863 - 6 - T; Univ. of Michigan, Ann Arbor.